I. Introduction

Catalysis by metalloenzymes occupies a relatively unique position when placed in the context of heterogeneous and homogeneous catalysis. For heterogeneous catalysis, it is difficult many times to obtain information on the number and types of atoms at the "active site" of the catalyst. For enzymic catalysis, a distinguishing feature is that even if one tends to focus on the metal ion as essential to the catalytic center, unique information can be obtained about changes at this one center in spite of the fact that the metal ion is bound to a large protein molecule of molecular weight from 6000 in the simplest cases to over 600,000 in the more complex metalloenzymes.

The primary, secondary, and tertiary structures of the macromolecule surrounding the metal ion, however, make possible an enormous variation in the microenvironment of the metal ion. The microenvironment also consists of amino acids whose side chains (and also perhaps the peptide backbone) can assume a role in a given catalytic reaction in addition to the metal ion. Such variation is not readily achieved in small molecular systems, but many variations in solvent polarity, pH, etc., can be applied to homogeneous catalysts.

The chemistry of the metalloenzymes must be considered as a special case of enzymic catalysis since most active sites of enzymes are stereospecific for only one molecule or class of molecules and many do not involve metal ions in catalysis. Since the metal ion is absolutely essential for catalysis in the examples chosen for this review, the mechanisms undoubtedly involve the metal ion and a particular protein microenvironment or reactive group(s) as joint participants in the catalytic event. It is our belief that studies of catalysis by metalloenzymes will have as many, if not more, features characteristic of protein catalysis in general, in a fashion similar to metal ion catalysis, and these studies will be directly applicable to heterogeneous and homogeneous catalytic chemical systems where the metal ion carries most of the catalytic function.

Numerous experimental techniques have been applied to study enzymes that possess a metal ion at the catalytic region in the protein molecule (*1–3*). These techniques for determining structure include nuclear magnetic resonance (NMR), electron paramagnetic resonance (EPR), fluorescence, and x-ray crystallography. Kinetic approaches have been used extensively to study the order of binding of substrates and the release of products. Rapid kinetic techniques are useful in determining individual rate constants. In this review we have chosen enzymes for which many independent experimental approaches have been utilized to obtain the coordinates in space of substrate atoms, metal ions, and various atoms of the protein that are involved in binding and catalysis. With these examples both structure and function have

been studied at the atomic level and provide the insight necessary for a complete understanding of the tremendous catalytic behavior of enzyme molecules.

The distinction between metalloenzymes and metal ion-activated enzymes is an empirical one. If an isolated enzyme contains a tightly bound metal ion that remains bound to the protein through purification, then the enzyme is designated a metalloenzyme. Metal ion-activated enzymes are often inactive after purification, but regain activity when the appropriate metal ion is added back.

It is possible in many metalloenzymes to substitute the native metal ion with another first transition ion either by removing the original ion with chelating agents or by exchange dialysis. In addition to certain interesting physical properties that can be studied by this method, an opportunity is provided to discover what kind of specificity for catalysis resides in the electronic properties of the metal ion. Studies of this type have been conducted with several metalloenzymes.

Metalloenzymes or metal ion-activated enzymes catalyze an enormous variety of organic reactions that are not restricted to any particular reaction class, but appear as catalysts for all types of reactions. Thus neither the presence of the metal ion nor the reaction type seems to be restrictive as far as metal-assisted enzyme catalysis is concerned. In some cases the metal ion appears to function as an electron acceptor or donor, but flavin cofactors have substituted as redox centers during evolution in some enzymes.

There is now considerable evidence that indicates that metal ion-activated enzymes and metalloenzymes catalyze reactions via ternary complexes consisting of a 1:1:1 ratio of enzyme:metal ion:substrate. Three coordination schemes are possible:

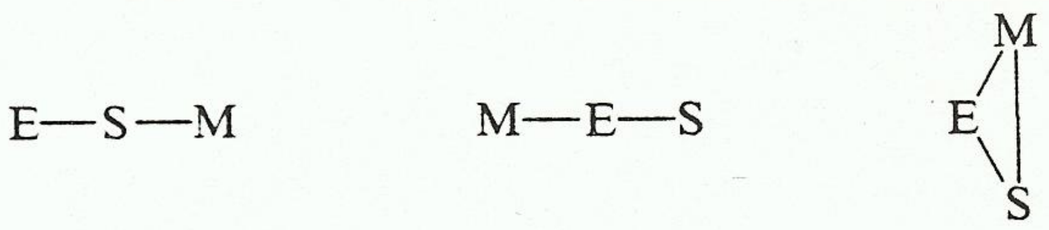

I II III

These involve the substrate bridge complex (I) wherein the metal ion is not bound to enzyme residues, the enzyme bridge complex (II) in which the metal ion is not involved in bond-making or -breaking steps (or for that matter substrate binding), and the metal ion bridge complex (III). For metalloenzymes the substrate bridge complex is not possible by definition. The metal ion bridge complex must have the substrate bound to the enzyme because all enzymic reactions are stereospecific and the chirality of a reaction could only reside in the substrate molecule and the enzyme groups.

To understand an enzyme mechanism thoroughly, which involves a

metalloenzyme or a metal ion-activated enzyme, the following points must be known: (1) the affinity of substrates, coenzymes, and cofactors, (2) the rate constants for each step, (3) the three-dimensional geometric relationship among the substrates, coenzymes, cofactors, and catalytically important residues of the enzyme, and (4) the chemical mechanism for each step; i.e., the electronic and atomic rearrangements. Many aspects of points (1)–(3) can be answered by magnetic resonance techniques (NMR, EPR, ENDOR), magnetic circular dichroism, rapid flow kinetics, and x-ray crystallography. Thus, a wide variety of physical techniques can be utilized to understand structure–function relationships in enzymology. The nature of the chemical mechanism (bond making and breaking steps) can be investigated in select cases by studying kinetic and thermodynamic isotope effects when "heavy" isotopes replace normal isotopes in substrate molecules (^{3}H or ^{2}H for ^{1}H, ^{13}C for ^{12}C, ^{15}N for ^{14}N, ^{18}O for ^{16}O, etc.). Chemical modifications of specific amino acids can be useful in determining if these residues are involved in binding substrates or metal ions. Enzymes can therefore be studied in macroscopic and microscopic detail by almost every technique available to scientists.

The following detailed discussion of three enzymes that have metal ions at their active sites will point out the current state of the art of enzymologists' understanding of enzymic catalysis. The examples have been chosen to include the most advanced use of stereochemical techniques, kinetic methodology, solution structural data (NMR, EPR, fluorescence energy transfer), and x-ray crystallographic structures.

II. Thermolysin

A. Background

Thermolysin is a metalloenzyme isolated from *Bacillus thermoproteolyticus*. It is a heat-stable extracellular endopeptidase of molecular weight 34,600. The enzyme catalyzes the hydrolysis of peptide bonds that have the amino group as part of hydrophobic residues such as phenylalanine, isoleucine, or leucine.

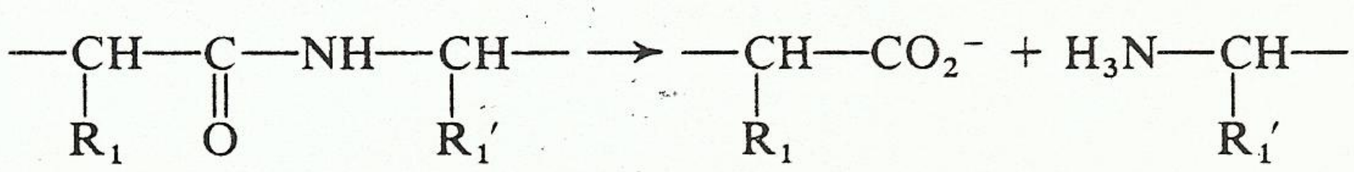

R_1 = phenylalanine(best)
R_1' = phenylalanine, isoleucine, leucine

Hydrolysis is fastest when both R_1 and R_1' are hydrophobic residues. Latt *et al.* (*4*) showed that the isolated enzyme has one Zn^{2+} and four Ca^{2+}.

The Zn^{2+} is required for catalysis, while the Ca^{2+} ions are necessary for thermostability.

This enzyme has been studied extensively by x-ray, kinetic, NMR, optical, circular dichroic, and fluorescence techniques. Thus, many approaches have been used to explore the role of the metal ions in catalysis and of other protein residues in substrate binding and catalysis. The review of this enzyme will serve to point out the information to be gained from using multiple biophysical approaches in understanding metalloenzyme catalysis.

B. Kinetic Studies

Thermolysin belongs to a class of proteases (called neutral proteases) which are distinct from the serine proteases, sulfhydryl proteases, metalloexopeptidases, and acid proteases. Neutral proteases A and B from *Bacillus subtilis* resemble thermolysin in molecular weight, substrate specificity, amino acid content, and metal ion dependence. Since physiological substrates are most likely proteins, it is difficult to design simple experiments that can be interpreted in terms of substrate specificity and relative velocities. Therefore, studies of substrate specificity and other kinetic parameters must be carried out on di- and tripeptides so that details of the mechanism of catalysis can be obtained and interpreted simply.

Most kinetic studies of enzymes are conducted under conditions where substrate concentration spans the upper and lower sides of the Michaelis constant, K_m. The most general form of kinetic expression for a one-substrate enzyme is given as

$$E + S \rightleftharpoons ES \rightarrow \text{product}$$

$$v = \frac{k_{cat}(E)(S)}{K_m + (S)}.$$

In kinetic studies with neutral proteases, the substrates are relatively insoluble and K_m values are generally high. For these enzymes, pseudo-first-order kinetic data can be obtained where $(S) \ll K_m$, leading to a rate expression, $v = k_{cat}(E)(S)/K_m$. Values of k_{cat}/K_m and K_m are measured and data compared for various substrates. Table I presents data at pH = 8 for a neutral protease from *B. subtilis* (*5*).

From these data one can see that the variation in K_m is small for the various dipeptide substrates that are amides ($-NH_2$), but that k_{cat}/K_m [proportional to $k/(E)$] values differ by almost 10^3. This indicates that the major change in catalysis is in the catalytic rate constant, k_{cat}, and that the side chains must bind differently to the enzymes to produce this effect.

The dipeptide Gly-Leu-NH_2 has a free α-amino group and $k/(E)$ is reduced about 10^2 over Z-Gly-Leu-NH_2. A free carboxyl in the substrate (Z-Gly-Leu)

TABLE I

Hydrolysis of Various Dipeptides by Neutral Protease

Substrate[a]	$k/(E) \times 10^4$, $S^{-1}(mg/ml)^{-1}$	$K_m \times 10^2$ (M)
Z-Gly-Ala-NH_2	0.43	1.04
Z-Gly-Val-NH_2	6.95	2.16
Z-Gly-Leu-NH_2	54.6	2.94
Z-Gly-Phe-NH_2	3.47	0.32
Z-Ala-Leu-NH_2	147.7	1.01
Z-Thr-Leu-NH_2	406.5	1.22
Gly-Leu-NH_2	≤ 0.51	—
Z-Gly-Leu	≤ 1.38	—

[a] *Z* is benzyloxycarbonyl. The -NH_2 represents the amide of the dipeptide. When -NH_2 is absent the dipeptide has a free carboxyl group, and when *Z* is absent the peptide has a free α-amino group.

lowers this value about 40-fold. This study establishes that the enzyme functions best with a bulky nonpolar substituent as amino acid side chain and that the active site will not accommodate charged groups in the peptide backbone or in the peptide chain.

The preceding study is directly applicable to understanding the active site of thermolysin, since a recent kinetic study (*6*) comparing neutral protease from *B. subtilis* with thermolysin showed that the two enzymes have identical pH rate profiles that peak near pH ~ 7.

C. Chemical Modification

Chemical modification studies of Pangburn and Walsh (*6*) and dipeptide inhibition studies of Feder *et al.* (*7*) led to the implication in catalysis of an enzymic group or groups with pK values around 7–8. To understand what group may be involved in binding and/or catalysis, one must know the primary sequence of the protein and then solve its x-ray structure. The amino acid sequences of neutral protease A and thermolysin have been reported (*8*, *9*) and a high degree of homology is evident.

As will be evident in the following section, histidine-231 is implicated in thermolysin catalysis by x-ray crystallographic studies. A plot of k_{cat}/K_m vs. pH for the substrate furylacryloylglycyl-L-leucinamide shows two breaks at pH 5.9 and 7.5, thus implicating two ionizable enzymic groups in catalysis. When histidine-231 is chemically modified by ethoxyformic anhydride, the enzyme is inactivated, suggesting that histidine is the enzymic group with pK = 7.5. The enzymic group with pK = 5.9 is most likely glutamic-143, which serves as a general base to aid in the deprotonation of a water molecule

for nucleophilic attack on the carbonyl of a peptide substrate (see the following section).

D. X-Ray Structure

Matthews and his collaborators have undertaken an x-ray study of crystalline thermolysin. Using the amino acid sequence and crystallographic data on the enzyme taken to a resolution of 2.3 Å (*10*), they have elucidated the native enzyme structure. Zn^{2+} is tetrahedrally coordinated by the enzyme and the four ligands are ring nitrogens of histidine-142 and -146, an oxygen of the γ carboxyl of glutamic-166, and an oxygen of a water molecule (Fig 1) (*10*). When the structure is determined in the presence of the dipeptide inhibitor β-phenylpropionyl-L-phenylalanine and the x-ray difference map is determined, the water molecule on the Zn^{2+} is displaced by the carbonyl of the dipeptide inhibitor. The structure of an enzyme–substrate complex is shown in Fig. 2, inferred from the inhibitor binding studies.

One salient feature of this model of the active site with a bound substrate is that the carbonyl of the peptide bond that is to be broken is coordinated to Zn^{2+}. This feature implies that the metal ion may serve as an electrophile to polarize the carbon–oxygen bond, thereby rendering the carbon succeptible to nucleophilic attack by water. In the x-ray structure a water molecule is

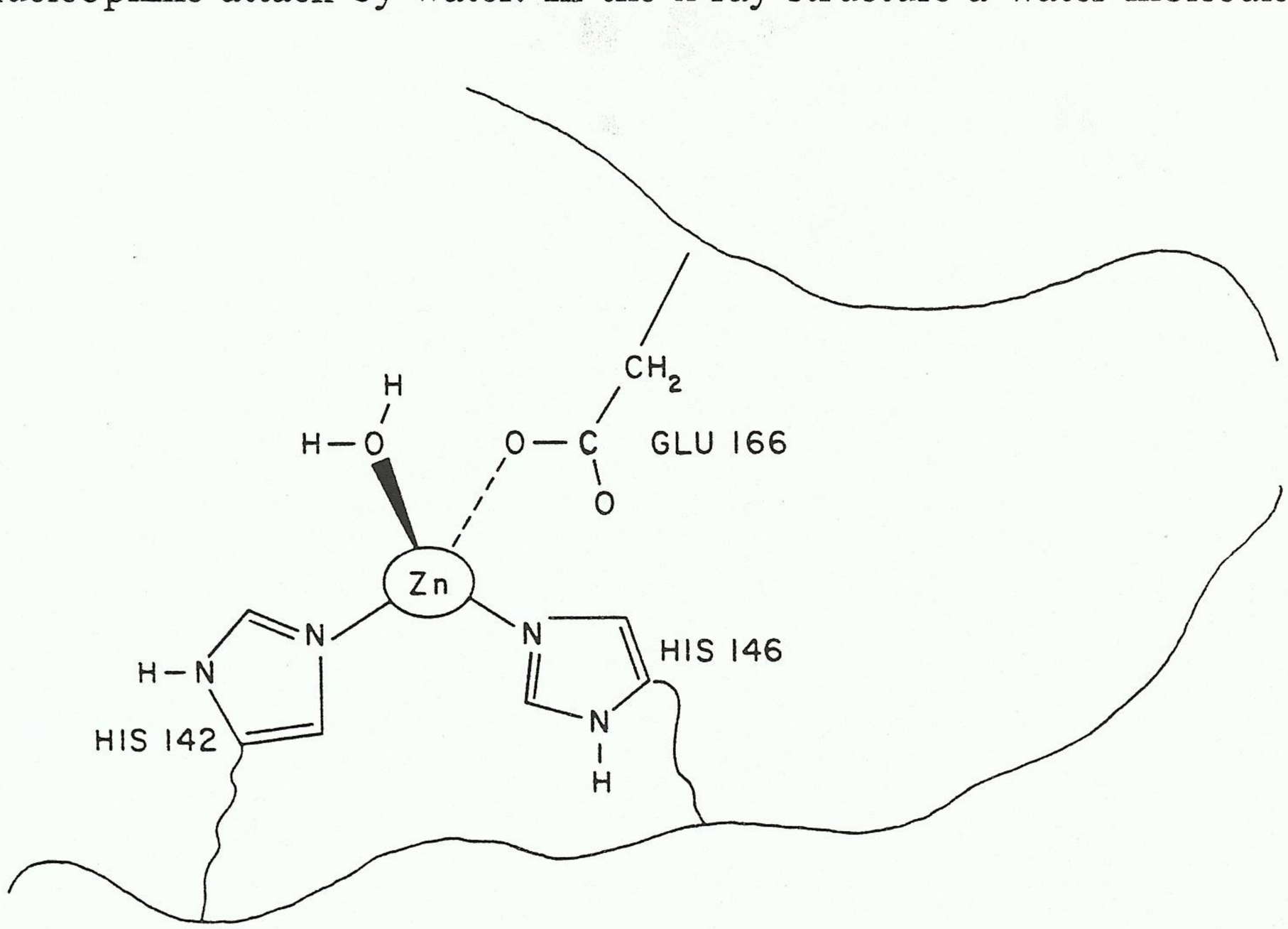

THERMOLYSIN ACTIVE SITE

FIG. 1. The zinc site of thermolysin. Data adapted from Kester and Matthews (*10*).

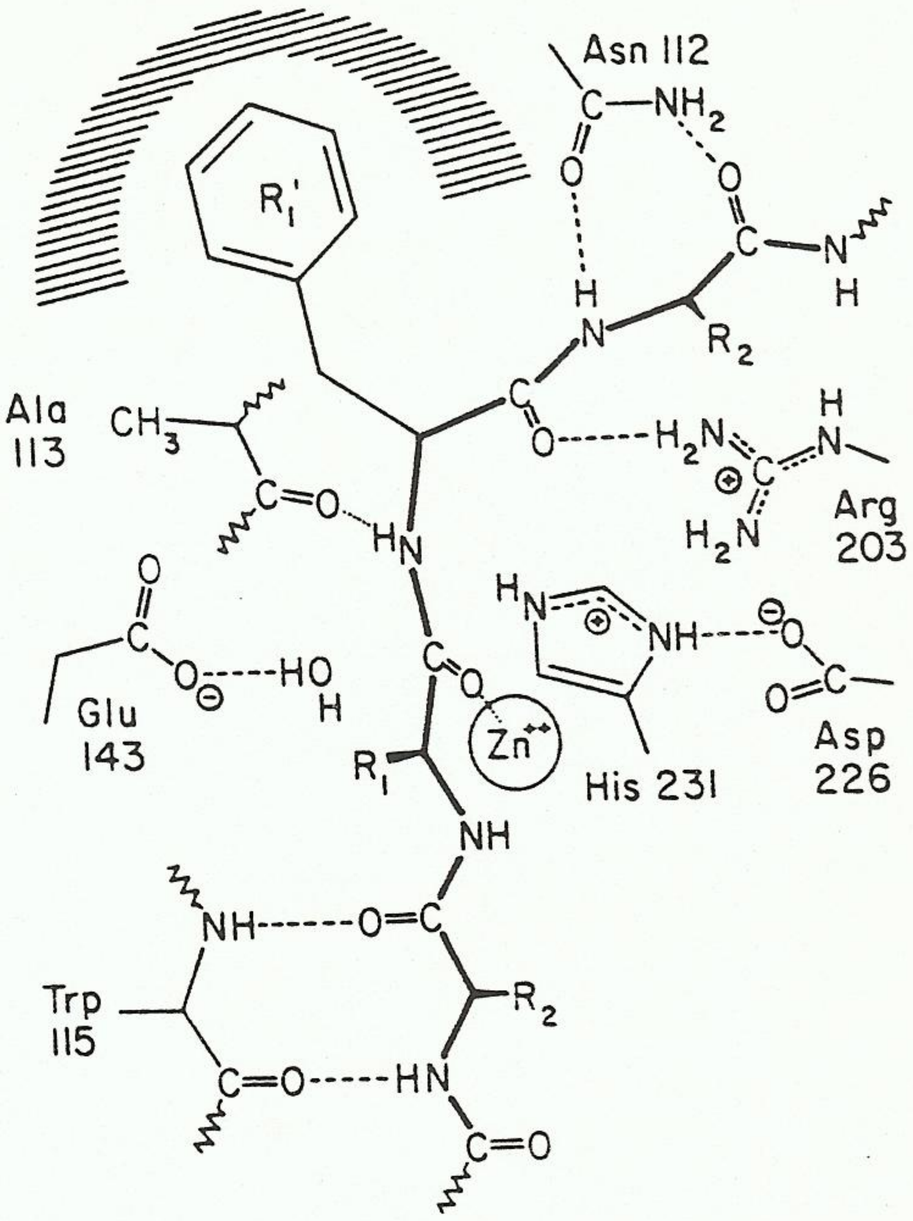

FIG. 2. Thermolysin active site. The structure shown is of a substrate bound to the active site Zn^{2+} and amino acid residues. From Kessler and Matthews (*10*). Reprinted with permission of The American Chemical Society.

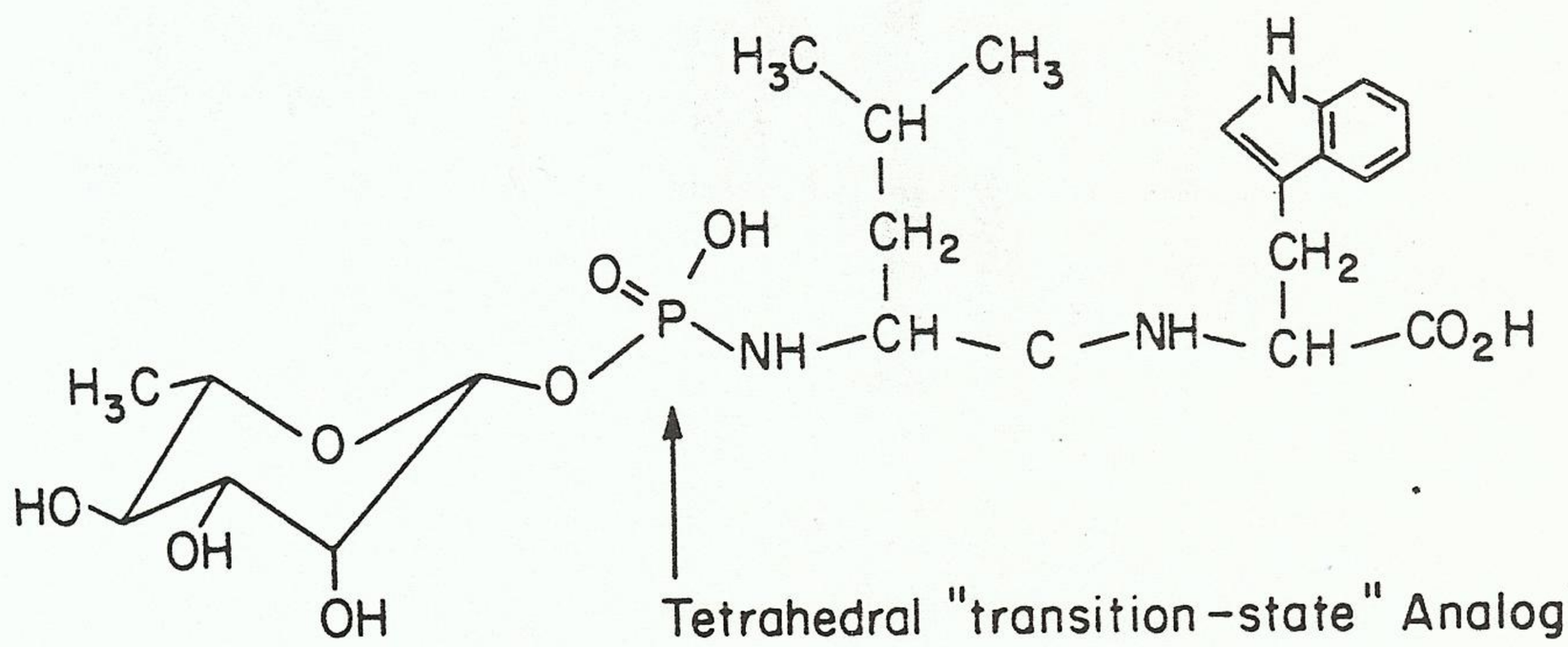

FIG. 3. Structure of the inhibitor phosphoramidon. The tetrahedral phosphorus atom binds at the active site of thermolysin and mimics the transition-state complex.

hydrogen-bonded to the γ-carboxyl of glutamic acid 143. Glutamic-143 can remove a proton from water, thereby aiding the nucleophilic attack. Another enzyme residue, histidine-231, is near the peptide nitrogen and can protonate this nitrogen during catalysis.

Further x-ray studies were conducted with an inhibitor that has a tetrahedral phosphorus atom where the carbonyl of the peptide bond would be located (*11*). The structure of this inhibitor, phosphoramidon, is given in Fig. 3. This compound binds to the enzyme about 10^5-fold better than other dipeptide inhibitors that have been studied (phosphoramidon, K_I =

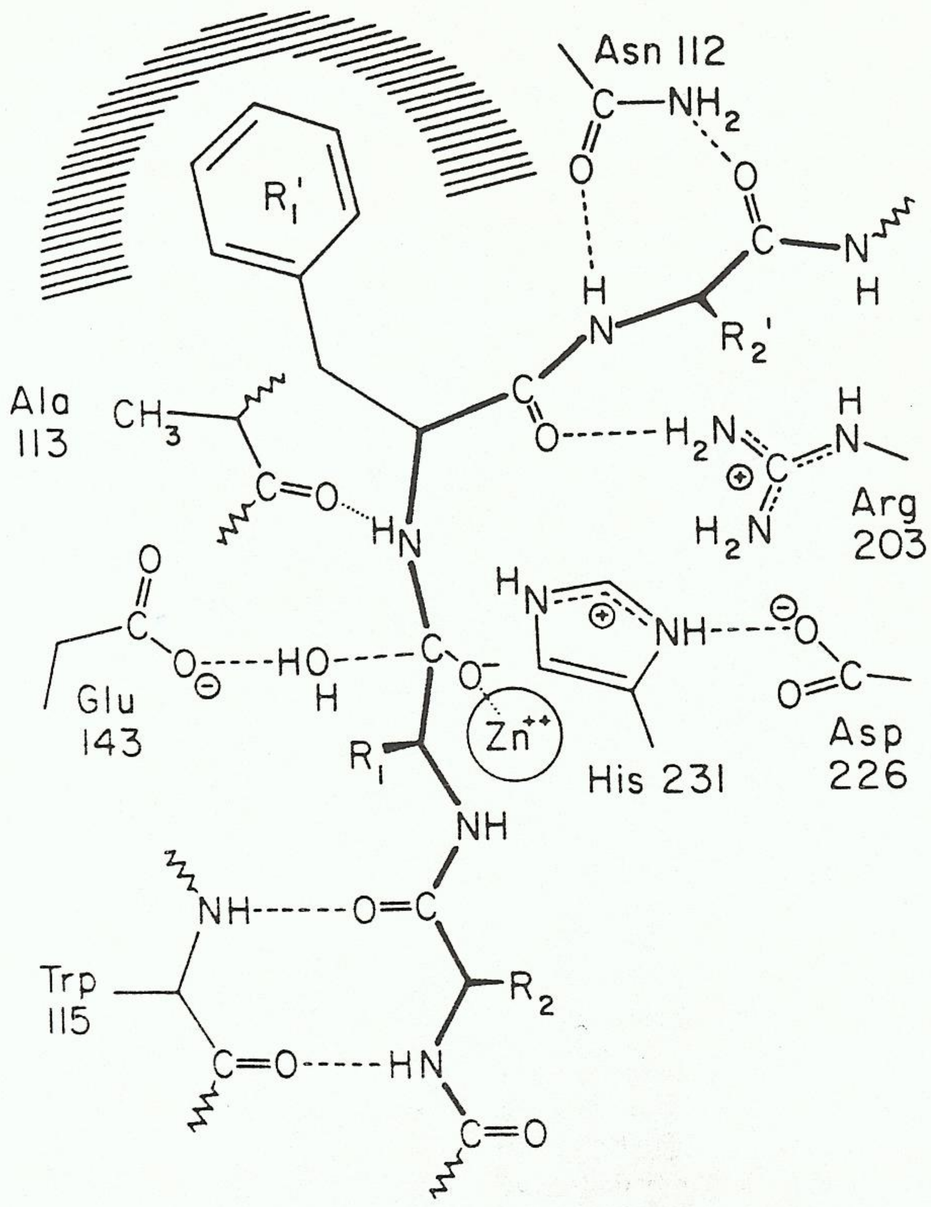

FIG. 4. Proposed transition-state structure for an enzyme-substrate complex with thermolysin. From Kessler and Matthews (*10*). Reprinted with permission of The American Chemical Society.

2.8×10^{-8} *M*; β-phenylpropionyl-L-phenylalanine, $K_I = 1.6 \times 10^{-3}$ *M*). This inhibitor can be considered a good "transition-state" analog of the thermolysin catalyzed reaction.

The x-ray difference map shows that the tetrahedral phosphorus binds in the pocket occupied by the carbonyl of a dipeptide and that one phosphorus oxygen binds to the Zn^{2+} while another oxygen displaces the water bound to glutamic-143. The proposed transition-state structure for the catalytic reaction is given in Fig. 4.

Overall the mechanism of the thermolysin reaction including the role of the Zn^{2+} in catalysis is given in Fig. 5. This proposed mechanism is based on inhibitor data and x-ray structure determination.

E. Physical Studies of the Metal Ion Environment

1. *Absorption Studies*

Since Zn^{2+} has a full 3d shell of electrons (d^{10}), it is a colorless, diamagnetic metal ion. Replacement of Zn^{2+} by Co^{2+} (d^7) does not produce large

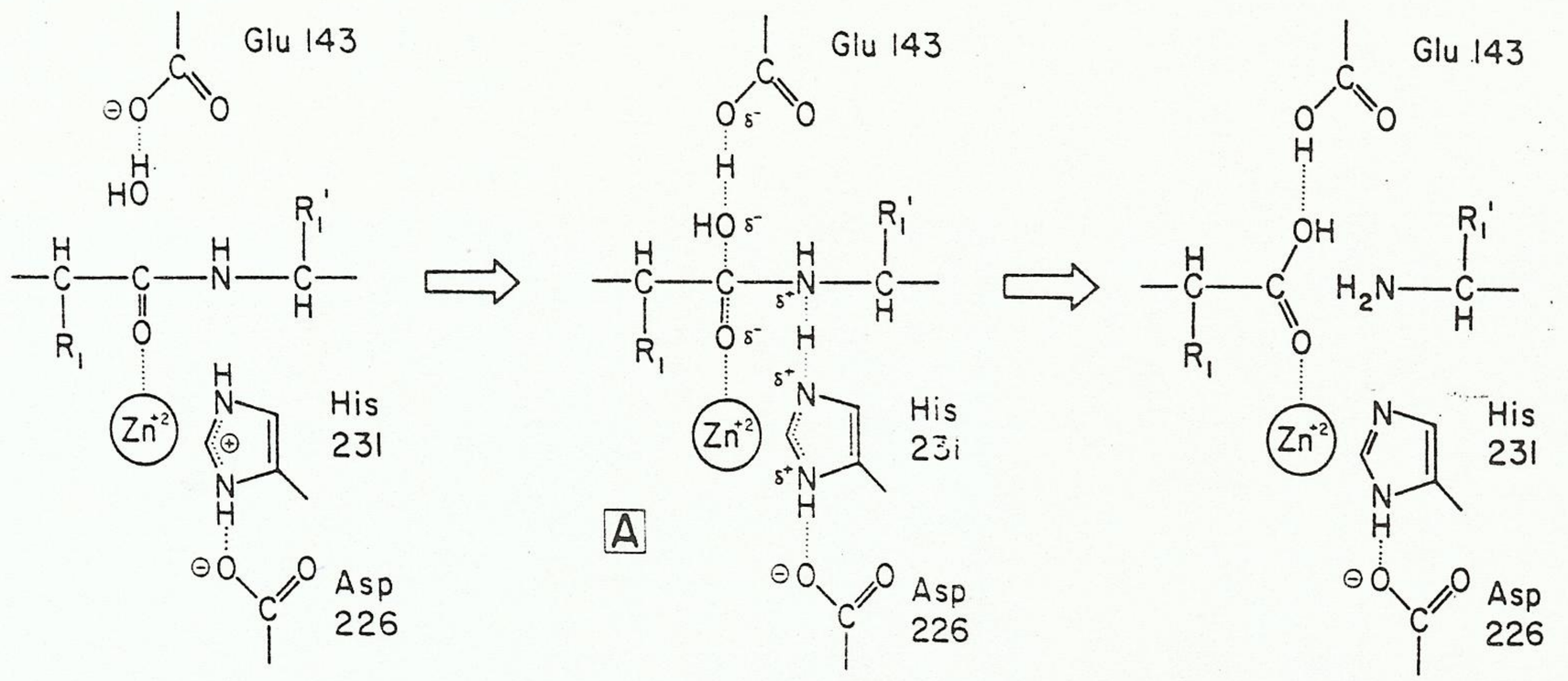

FIG. 5. Proposed mechanism of action of thermolysin showing the catalytically important residues.

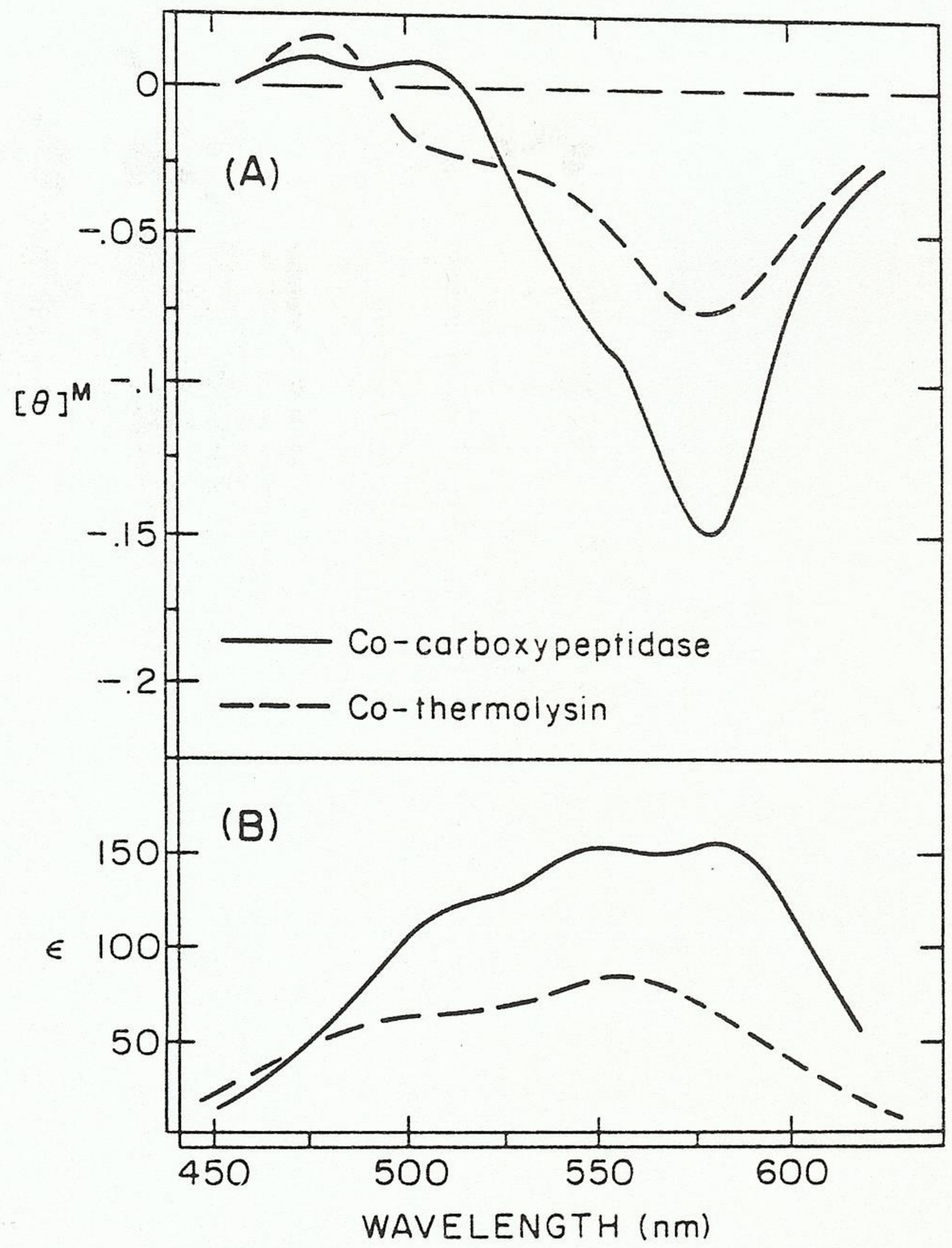

FIG. 6. Absorption and magnetic circular dichroism spectra of Co^{2+} thermolysin. (A) MCD spectra. (B) Absorption spectra.

alterations in the protein conformation or structure of thermolysin since the Co^{2+}-substituted enzyme is still catalytically active (*12*). With Co^{2+} one can study the absorption, circular dichroism (CD), magnetic circular dichroism (MCD), and EPR properties of enzyme-bound Co^{2+}. All of these techniques will provide information on the coordination environment of the metal ion and the changes in the environment upon addition of substrates or inhibitors. Figure 6 shows the absorption and MCD spectra of Co^{2+}–thermolysin (*13*). The addition of the inhibitor β-phenylpropionyl-L-phenylalanine produces a change in intensity of both the optical and MCD spectra. These changes suggest alteration of the coordination environment of bound Co^{2+}, and this would be consistent with displacement of the water molecule bound to Co^{2+} by oxygen of the carbonyl, as demonstrated in the x-ray study.

2. *Models for Metal Ion Site*

One would like to be able to deduce structural information from studies on the enzyme in solution rather than having to rely on the resolution of the complete x-ray structure of the enzyme. An approach to this problem is to synthesize model complexes, to measure their spectra, and to compare these to spectra from the enzyme complex. Ishly and Horrocks (*14*) have studied

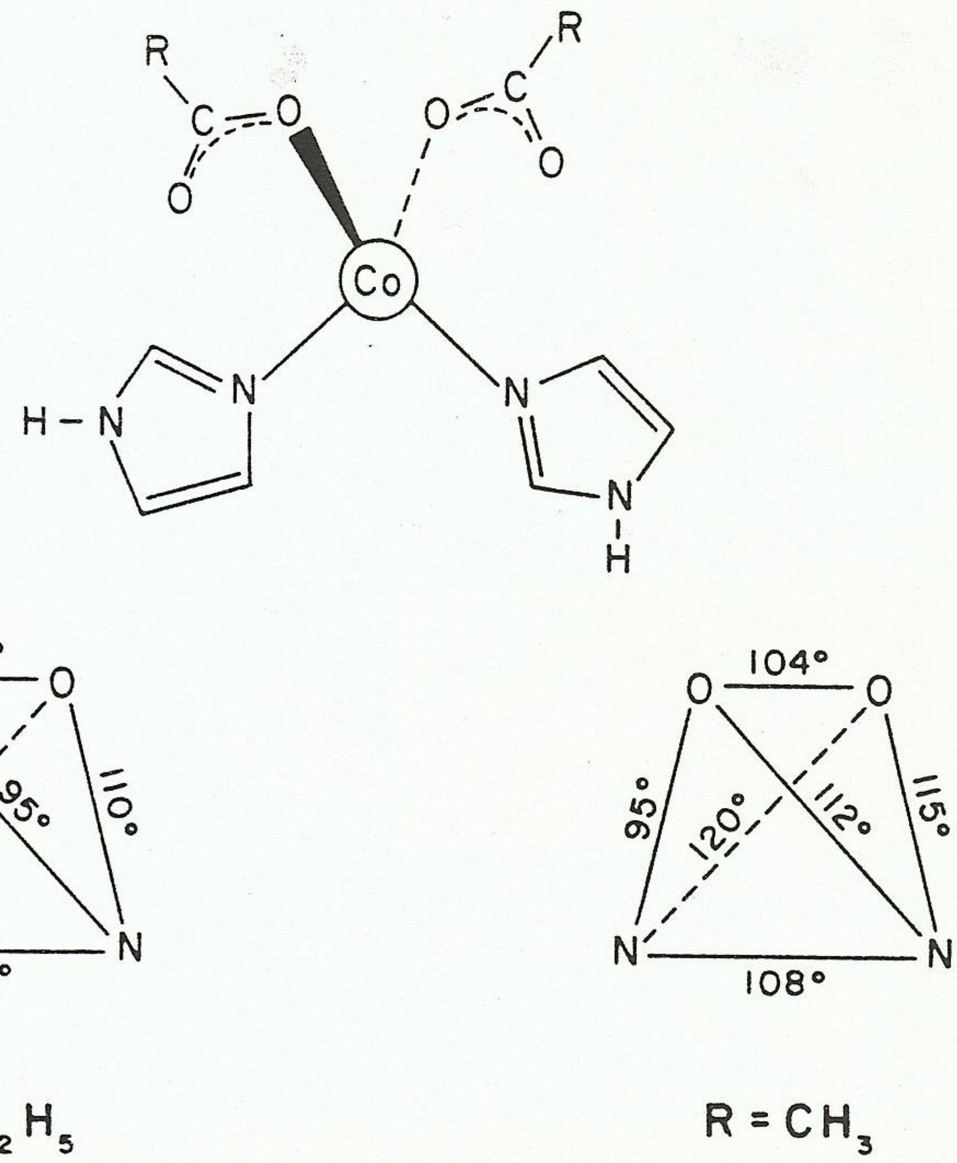

$R = C_2H_5$ $R = CH_3$

FIG. 7. Co^{2+} complexes with two oxygen and two nitrogen ligands that are models for the metal ion site of thermolysin.

the two complexes shown in Fig. 7 with two oxygen and two nitrogen ligands to Co^{2+}. One complex has two propionic acid residues, while the other has two acetate residues as oxygen ligands to Co^{2+}. The metal–ligand bond angles are given in the figure to emphasize the differences in these complexes.

Figure 8 shows the MCD spectra for these two complexes. The spectra of the model complexes resemble well the Co^{2+}–thermolysin spectra. Substitution of 2-methylimidazole for imidazole produces a spectrum similar to that for the Co^{2+}–thermolysin-β-phenylpropionyl-6-phenylalanine complex, while the spectrum with imidazole resembles closely that of the Co^{2+}–thermolysin spectrum without inhibitor.

Additional differences are noted in the EPR spectra of these two complexes (Fig. 9). The g anisotropy in the EPR spectra is different for the two complexes in spite of very small differences in their tetrahedral bond angles (Fig. 7). The EPR spectrum for the protein (*15*) does not have the excellent resolution of that of the model complexes and further studies may be necessary to demonstrate quantitative similarities between the model complexes and the enzyme–Co^{2+} complex.

3. *Other Studies of the Metal Ion Environments*

A novel approach for determining metal–metal distances in proteins in solution was applied to thermolysin by Horrocks *et al.* (*16*). As mentioned earlier, thermolysin has four Ca^{2+} binding sites. Three of the four can be replaced by trivalent lanthanide ions. Tb^{3+} fluorescence is enhanced when Tb^{3+} is bound to the so-called #1 Ca^{2+} site of thermolysin. When Co^{2+} is added to the Zn^{2+} active site, the fluorescence of bound Tb^{3+} is quenched by

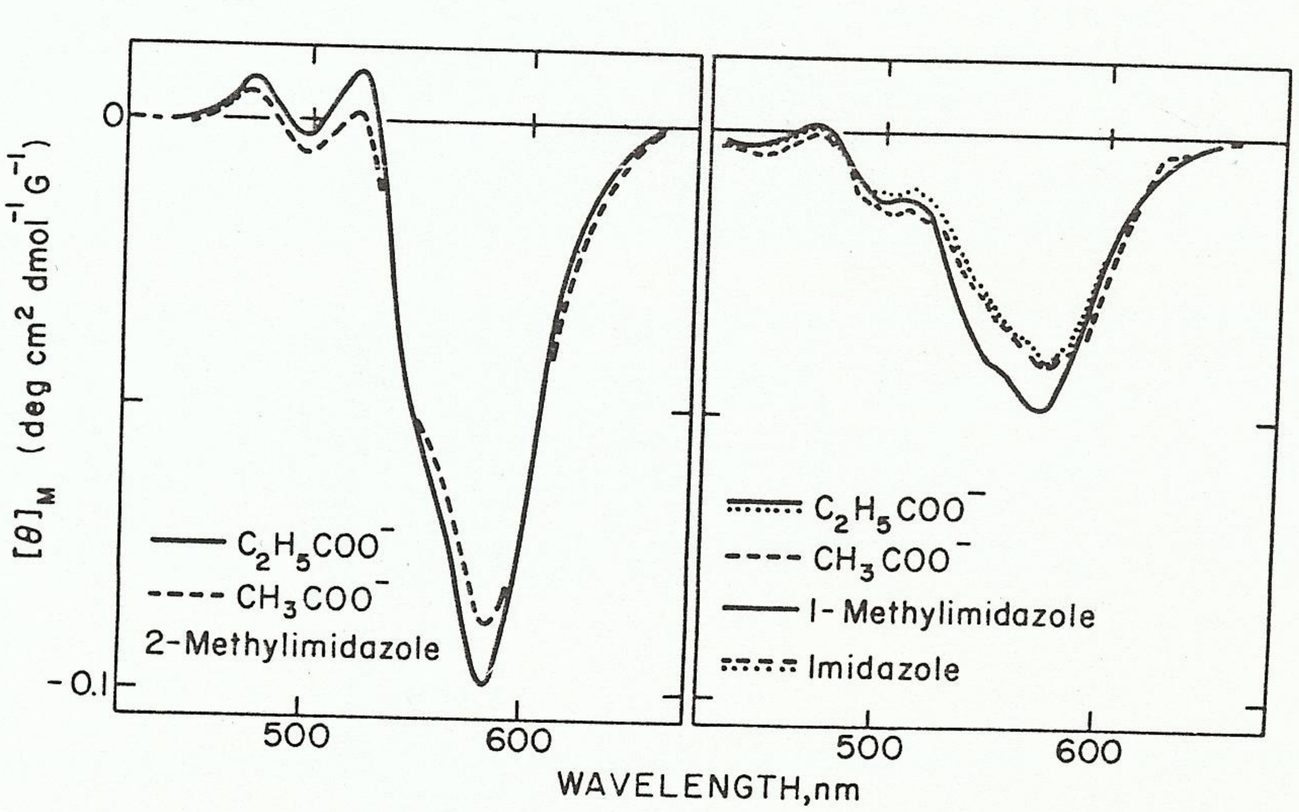

FIG. 8. Magnetic circular dichroism spectra of Co^{2+} complexes. The oxygen and nitrogen ligands are given for each complex.

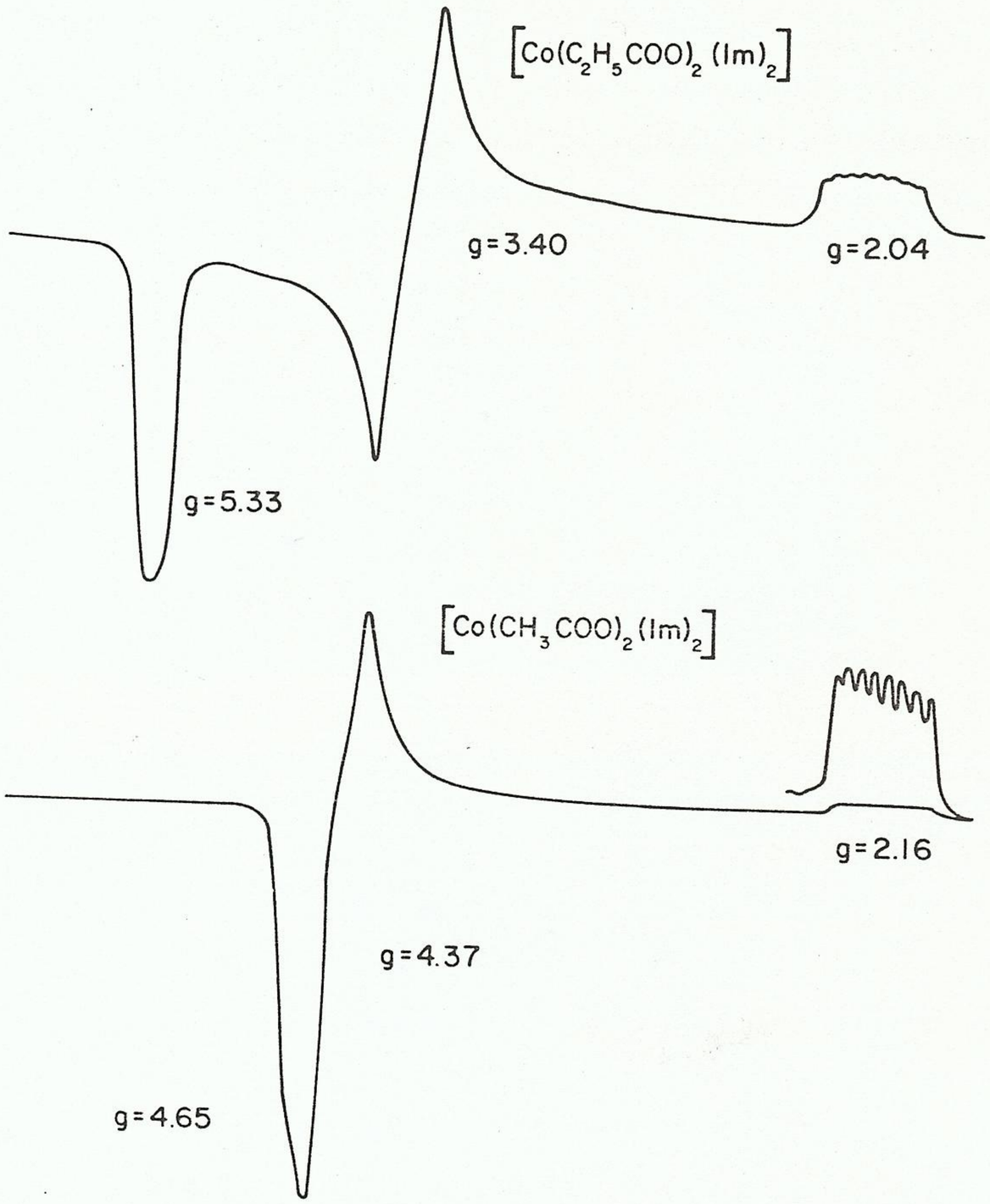

FIG. 9. Electron paramagnetic resonance spectra of Co^{2+} complexes in Fig. 7.

89%. Using the Förster energy transfer equations (*16*), one can calculate that Co^{2+} and Tb^{3+} are 13.7 Å apart, in excellent agreement with the value of 13.7 Å from the protein x-ray structure. This technique should be valuable for future applications to other multimetal ion binding proteins and enzymes.

Another technique that uses the fluorescence properties of trivalent lanthanides is that of the detection of fluorescence emission decay induced by pulsed dye laser excitation. Horrocks and Sudnick (*17*) have applied this technique to the study of water molecules bound to metal ions in small complexes and proteins. In one study they found that the exponential decay of Tb^{3+} fluorescence is altered when H_2O is replaced by D_2O and that this change can be used to determine the number of coordinated water molecules on the metal ion. With thermolysin, bound Tb^{3+} had 1–2 water molecules in the first coordination shell. This number is consistent with the x-ray structure.

NMR studies of protons of water also can be used to determine the number

of water molecules in enzyme–metal ion complexes, and this approach has been used with thermolysin. Bigbee and Dahlquist (*18*) found that there was one exchangable water molecule in a thermolysin–Mn^{2+} complex and that this water molecule appeared to be displaced (at least partially) by inhibitors. These results also are consistent with the x-ray data. These authors also studied inhibitor binding by ^{19}F-NMR (*19*). They concluded that the inhibitor *N*-trifluoroacetyl-D-phenylalanine binds to the enzyme at two sites, one of which is perhaps in the coordination sphere near the metal ion.

F. Conclusions

Overall, many biophysical approaches have been applied to the study of catalysis by the metalloenzyme thermolysin. The metal ion was found by all studies to be involved in binding substrates and inhibitors. In addition, the x-ray structure of the protein has been useful in reaching the conclusion that the metal ion probably functions in catalysis as an electrophilic "sink."

III. Yeast Hexokinase

A. Background

Yeast hexokinase catalyzes the following reaction:

$$\text{hexose} + \text{MgATP} \leftrightarrows \text{hexose-6}P + \text{MgADP} + H^+$$

This enzyme plays a key role in the metabolism of glucose and other related sugars. The physical and kinetic properties of yeast hexokinase have been extensively studied. Numerous recent studies have been made of its role in the phosphoryl transfer reaction.

Hexokinase has a molecular weight of 102,000 and is composed of two identical subunits of 51,000 molecular weight each (*20–22*). In yeast, hexokinase exists as a mixture of two isoenzymes (*23*). These forms have been named A and B (*23*). These isoenzymes can be separated by chromatography and have been found to be chemically different (*23*, *24*). Some of the earlier work with hexokinase was done with preparations that contained a mixture of isoenzymes. Work also was done with enzyme that was proteolytically modified. These variations undoubtedly have been responsible for some of the controversy concerning the properties of this enzyme.

Much of the earlier work on hexokinase has been summarized in two reviews that appeared in 1973 (*25*, *26*). The emphasis here will be on information that has appeared since that time. Significant advances have been made with respect to kinetic mechanism, stereospecificity of phosphoryl transfer, and x-ray structure.

B. Substrate Specificity

1. *Sugar Site*

Unlike many enzymes, hexokinase has a broad substrate specificity. A partial list of substrates for the sugar site is presented in Table II. Structures for some of these compounds are given in Fig. 10. It should be pointed out that kinetic constants for the various substrates were obtained under a variety of conditions with different forms and modifications of the enzyme.

From the list of substrates in Table II (*27–33*) it is apparent that the orientations of the hydroxyls on carbons 3 and 4 of glucose(I) are important for binding and activity, since neither D-allose(II) nor D-galactose(III) are very good substrates. The position of the hydroxyl at carbon 2, however, is relatively unimportant, since D-mannose(IV) and other compounds modified at this carbon are very good substrates. 1,5-Anhydro-D-glucitol(V) and 1,5-anhydro-D-mannitol(VI) are substrates that lack the anomeric hydroxyl and thus are locked into a pyranose configuration. The low activity seen with these compounds suggests that the anomeric hydroxyl is important for binding to the enzyme. However, the anomeric hydroxyl can be in either

TABLE II

Kinetic Constants for the Sugar Substrates of Yeast Hexokinase

Substrate	K_m, mM	Relative V_{max}	Reference
D-Glucose	0.01	100	*27*
D-Galactose	>50	>0.2	*27*
D-Allose	>100	>10	*27*
D-Mannose	0.05	80	*27*
2-Deoxy-D-glucose	0.30	100	*27*
D-Glucosamine	1.50	70	*27*
D-Glucosone	0.02	20	*27*
5-Thio-D-glucose	4.0	1	*28*
2-Deoxy-2-fluoro-D-glucose	0.19	50	*29*
2-Deoxy-2-fluoro-D-mannose	0.41	85	*29*
3-Deoxy-3-fluoro-D-glucose	70	10	*29*
4-Deoxy-4-fluoro-D-glucose	84	10	*29*
1,5-Anhydro-D-glucitol	3	1	*27*
1,5-Anhydro-D-mannitol	7	6	*30*
D-Fructose	7	180	*27*
2,5-Anhydro-D-mannitol	6.3	155	*31*
2,5-Anhydro-D-glucitol	47	109	*31*
2,5-Anhydro-D-mannose	0.31	109	*31*
1-Deoxy-D-fructose	614	2[a]	*32*
5-Thio-D-fructose	1.7	2.6	*33*

[a] Relative to fructose.

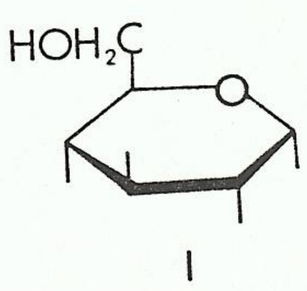

I

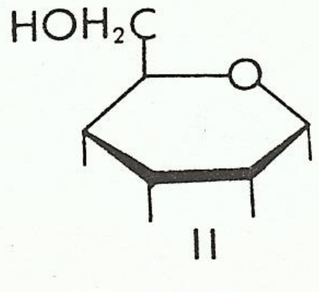

II

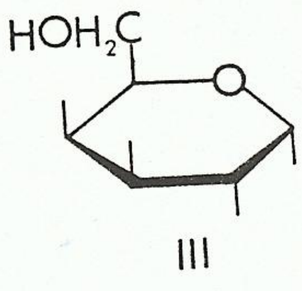

III

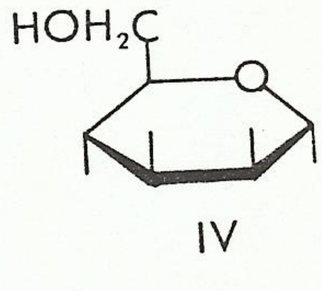

IV

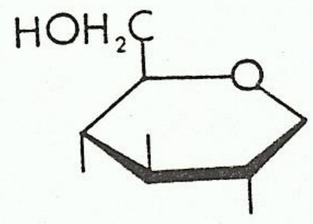

V

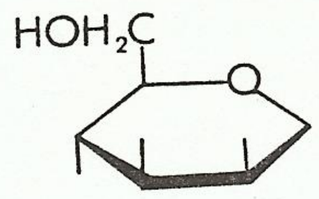

VI

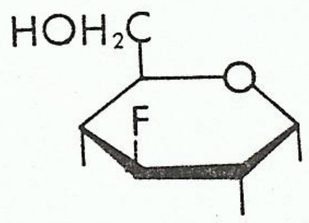

VII

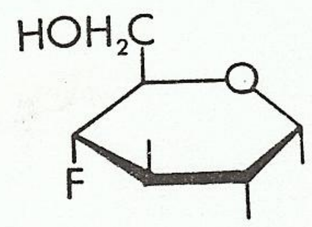

VIII

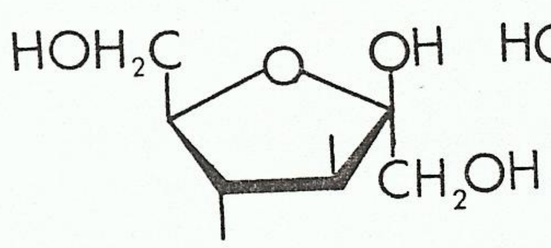

IX

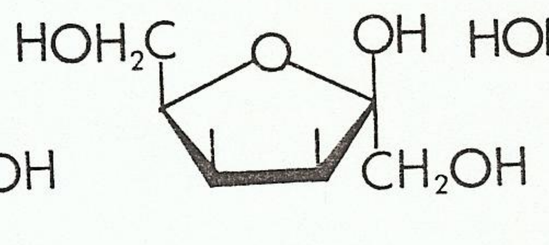

X

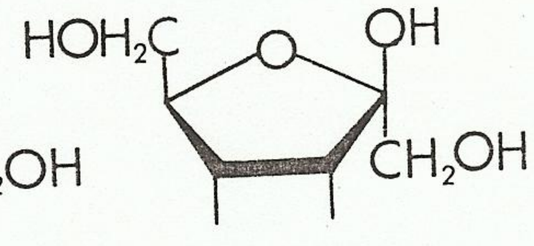

XI

FIG. 10. Structures of sugars and sugar analogs that have been tested as substrates for yeast hexokinase.

the α or β configuration since both α-D-glucose and β-D-glucose are substrates (*34–36*). The rate with α-D-glucose is 1.2–1.5 times faster than with β-D-glucose (*34–36*). Since neither 3-deoxy-3-fluoro-D-glucose(VII) nor 4-deoxy-4-fluoro-D-glucose(VIII) are good substrates, this suggests that the hydroxyls at carbons 3 and 4 are acting as proton donors rather than proton acceptors in the formation of hydrogen bonds to enzyme (*10*).

Hexokinase will also phosphorylate D-fructose(IX) and fructose analogs. This shows that the enzyme also will accept furanose rings at the active site. The same hydroxyls appear to be important for binding and activity since D-tagatose(X) and D-psicose(XI), the C-4 and C-3 epimers of fructose, are not substrates for hexokinase (*37*).

2. *Nucleotide Site*

A partial list of substrates that serve as phosphoryl donors are presented in Table III (*38–42*). Alterations have been made in the base, sugar, and phosphate portions of ATP. The amino group at position 6 appears to be relatively unimportant since a large number of bulky substituents can be attached here with little effect on binding or activity (*38–40*). It can also be removed since purine riboside-5′-triphosphate is a good alternate substrate (*38*). Replacement of the amino group with a hydroxyl group (ITP) greatly increases the K_m, but only reduces the V_{max} about 50% (*40*). The high activity of 7-deazaadenosine-5′-triphosphate indicates that the nitrogen at position 7 is not in strong interaction with the enzyme (*40*). Both of the ribose hydroxyls appear important for good activity since removal of either increases the K_m about sixfold and decreases the V_{max} by a factor of 16 (*40*).

C. Stereochemistry of the Active Complex of MgATP

Cornelius and Cleland have recently determined the absolute stereochemistry of the Mg^{2+} complex of ATP that is active with yeast hexokinase (*43*). MgATP can exist in solution as a pair of bidentate diastereomers (monodentate and tridentate complexes can also exist). The two possible bidentate isomers are shown schematically in Fig. 11. The two configurations have been labeled Λ and Δ (*44*). There are also four possible tridentate isomers.

TABLE III

Kinetic Constants for the Nucleotide Substrates of Yeast Hexokinase

Substrate	K_m	Relative V_{max}	Reference
Adenosine-5′-triphosphate	0.100	100	*38*
N^6-Benzoyladenosine-5′-triphosphate	0.046	56	*39*
N^6-Monomethyladenosine-5′-triphosphate	0.13	83	*40*
Guanosine-5′-triphosphate	0.34	2	*40*
Purine riboside-5′-triphosphate	0.60	53	*38*
2-Aminopurine riboside-5′-triphosphate	0.34	2	*40*
2,6-Diaminopurine riboside-5′-triphosphate	7.46	11	*40*
8-Bromoadenosine-5′-triphosphate	0.032	40	*38*
2′-Deoxyadenosine-5′-triphosphate	0.57	6	*40*
3′-deoxyadenosine-5′-triphosphate	0.59	6	*40*
7-Deaza-adenosine-5′-triphosphate	0.18	94	*40*
Adenosine-5′-(1-thiotriphosphate)	1.2	28	*41*
Adenosine-5′-(2-thiotriphosphate)	ND[a]	ND	*42*

[a] ND, not determined.

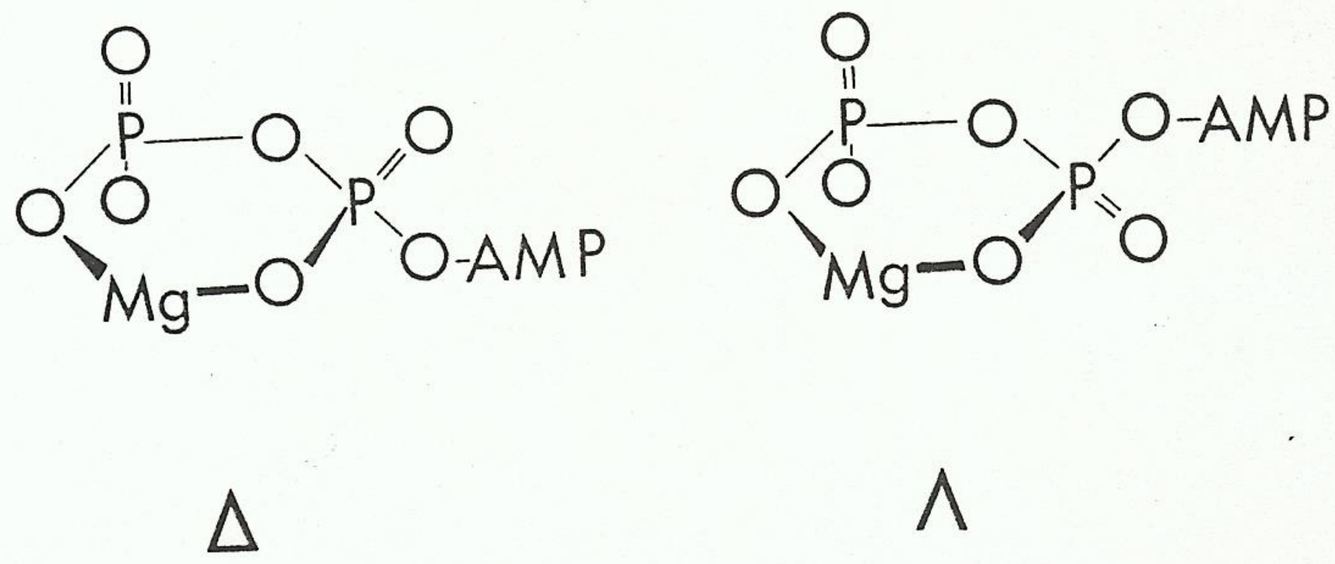

Δ Λ

FIG. 11. Structures of the two β,γ-bidentate diastereomers of MgATP.

Which of the two possible isomers is active with yeast hexokinase? Since Mg^{2+} exchanges ligands rapidly, it is not possible to separate the two species (*45*). Cornelius and Cleland synthesized $Co(NH_3)_4ATP$, which is bidentate and, since Co^{3+} exchanges ligands very slowly, the individual isomers should be stable to isomerization (*46*). $Co(NH_3)_4ATP$ was found to be a substrate for hexokinase in the following reaction (*43*):

$$\text{D-Glc} + Co(NH_3)_4ATP \rightarrow Co(NH_3)_4(Glc{-}6{-}P)ADP$$

The glucose-6-*P* remains in the coordination sphere of the cobalt. Only one-half of the mixture of the two isomers was a substrate; the part remaining was inert, although it did inhibit. The inert material and the product were separated and a degradation product of the inert material was crystallized. The absolute stereochemistry was determined by x-ray crystallography (*44*). The active isomer of $Co(NH_3)_4ATP$ used by hexokinase was found to correspond to the Λ isomer of β,γ-bidentate MgATP (*43*).

Jaffee and Cohn have used the above information to assign the absolute configuration to the two isomers of adenosine-5′-(2-*O*-thiotriphosphate) (*42*). Since the β-*P* of ATP is prochiral, the introduction of a sulfur as a replacement for one of the nonbridge oxygens results in a pair of diastereomers. These diastereomers have been labeled A and B by Eckstein and Goody (*47*). Jaffee and Cohn found that only the B isomer of adenosine-5′-(2-*O*-thiotriphosphate) was a substrate for hexokinase and thus, by analogy with the results of Cornelius and Cleland, the B isomer has the structure shown in Fig. 12 (*42*). The Mg^{2+} is presumed to be binding to oxygen rather than sulfur because of the known preference of Mg^{2+} for oxygen over sulfur (*48*). When the Mg^{2+} was replaced by Cd^{2+}, hexokinase was specific for the A isomer of adenosine-5′-(2-*O*-thiotriphosphate) (*42*). This occurs because cadmium greatly prefers to coordinate through the sulfur atom rather than the oxygen atom (*48*, *49*). The active species still corresponds to the Λ isomer of β,γ-bidentate MgATP, as shown in Fig. 13. Hexokinase has also been found to use predominantly the A isomer of adenosine-5′-(1-*O*-thiotriphosphate) (*41*). The absolute configuration of the two isomers recently has

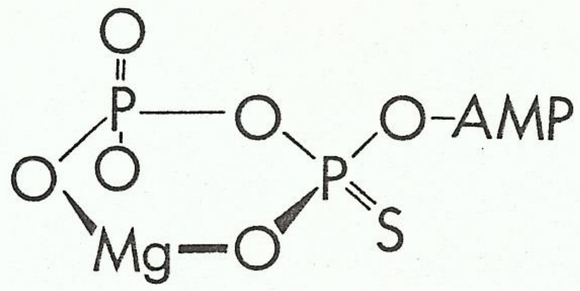

FIG. 12. Structure of the Mg^{2+} complex of the B isomer of adenosine-5′-(2-*O*-thiotriphosphate).

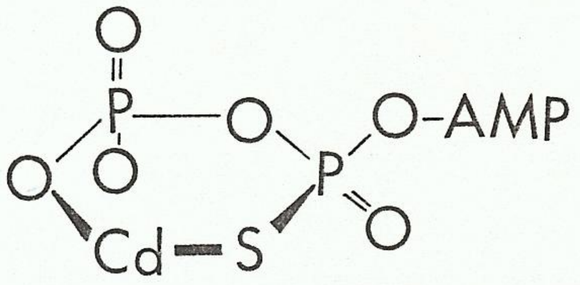

FIG. 13. Structure of the Cd^{2+} complex of the A isomer of adenosine-5′-(2-*O*-thiotriphosphate).

been determined. The A isomer has the *S* configuration and the B isomer has the *R* configuration (*50*, *51*).

D. KINETIC MECHANISM

1. *Introduction*

In the last 15 years a large number of publications have been concerned with the determination of the kinetic mechanism of yeast hexokinase. Unfortunately, there has been much disagreement between various authors on the conclusions to be drawn from such studies.

In a two-substrate reaction similar to that catalyzed by hexokinase, two basic mechanisms may be at work. First, a "ping-pong" reaction may be occurring in which the enzyme shuttles between a stable enzyme intermediate, such as a phosphorylated enzyme, and a free enzyme. Second, the reaction may be sequential, in which case no reaction occurs until both substrates are on the enzyme. There are two types of sequential mechanisms. If one substrate cannot bind until after the addition of the other substrate the mechanism is said to be ordered. However, if they can combine in any order the mechanism is said to be random. The various kinetic methods for distinguishing between these mechanistic forms have been summarized by Cleland (*52*). The evidence for and against these possible kinetic schemes will now be summarized for yeast hexokinase.

2. *Initial Velocity Studies*

A number of initial velocity studies have been made with yeast hexokinase. All results to date indicate an intersecting initial velocity pattern in

both the forward and reverse reactions (*53–55*). This indicates that hexokinase has a sequential kinetic mechanism. Thus, the possibility that ATP phosphorylates the enzyme, which in turn phosphorylates glucose, is excluded as being kinetically important.

3. *Product Inhibition Studies*

Since the mechanism is sequential, product inhibition studies have been used to try to determine whether the mechanism is ordered or random. These results have been contradictory and have varied from laboratory to laboratory. Rudolf and Fromm (*56*) found that glucose-6-*P* was a noncompetitive inhibitor versus either glucose or MgATP. MgADP was also noncompetitive versus MgATP or glucose. However, Noat *et al.* found that glucose-6-*P* was competitive versus glucose and noncompetitive versus MgADP, while MgADP was noncompetitive versus both glucose and MgATP (*55*). Kosow and Rose have shown that MgADP is noncompetitive with respect to MgATP at low MgADP concentrations, but competitive at high concentrations (*57*). Noat *et al.* argue that their data support an ordered reaction mechanism in which glucose adds before MgATP, followed by the ordered release of MgADP and Glc-6-*P* (*55*). Fromm and co-workers argue that the mechanism is actually random, but they must postulate a number of abortive complexes with certain sets of rate constants to make their data compatible with the usual results seen for a random mechanism (*54*, *56*). On the basis of their results, Kosow and Rose have argued that the release of products is random, but that there is a preferred pathway in which MgADP leaves before Glc-6-*P*. They also state that the release of Glc-6-*P* from the enzyme–(Glc-6-*P*) complex is at least partially rate limiting for the reaction (*57*).

4. *Isotope Exchange at Equilibrium*

Fromm *et al.* measured the ATP $\leftrightarrow$ ADP and Glc $\leftrightarrow$ Glc-6-*P* isotope exchange at equilibrium (*58*). They found that both exchange rates increased and then leveled off to a plateau as the level of ATP/ADP or Glc/Glc-6-*P* was raised (*58*). No inhibition was seen of either exchange (*58*). These results are in agreement with a random mechanism and not with an ordered one. However, both exchange rates were not the same. The MgATP $\leftrightarrow$ MgADP exchange was about 50% faster than the Glc $\leftrightarrow$ Glc-6-*P* exchange (*58*). This indicates that the exchange is partially limited by the release of glucose and/or glucose-6-*P* from the enzyme. If the mechanism was strictly ordered as postulated by Noat *et al.*, the Glc $\leftrightarrow$ Glc-6-*P* exchange would have been inhibited at high concentration of MgATP/MgADP (*52*).

5. *ATPase Reaction*

In the absence of added glucose, hexokinase was found to catalyze the very slow hydrolysis of MgATP (*59*). This has been explained by assuming that water has replaced glucose at the active site of the enzyme. This ATPase activity can be inhibited by compounds that inhibit the hexokinase activity (*60*) and can be stimulated by compounds such as D-xylose or D-lyxose which lack the terminal -CH_2OH of glucose (*61*). The ATPase reaction has been used to support evidence that hexokinase has a random kinetic mechanism, since it shows that ATP can bind to hexokinase in the absence of glucose (*62*).

6. *Binding Studies*

Binding studies have shown that hexokinase will bind one glucose molecule per subunit (*63*). Direct binding studies with ATP could not be determined since its binding constant is apparently too high (*64*).

7. *Isotope Partitioning Experiments*

Rose *et al.* (*65*) have recently introduced a method for determining the rates of release of substrates from the various enzyme forms relative to the overall turnover of the enzyme. This is done by incubating hexokinase with enough radioactive glucose so that all of the enzyme is complexed with substrates. This solution is then added to a solution containing a large excess of unlabeled glucose and various amounts of MgATP and then rapidly quenched with acid. The glucose-6-*P* that is formed is isolated and, from its specific activity, the amount of initially bound glucose that proceeds to form the product, as opposed to that dissociating into the pool of unlabeled glucose is determined. From the percentage of initially bound glucose that is trapped, the kinetic constant for MgATP, and using the appropriately derived equations, the rate of release (K_{off}) of glucose from the E-glucose and E-glucose-MgATP complexes can be determined (*65*). They found that glucose did not dissociate from the E-glucose–MgATP complex to any extent and K_{off} from E-glucose was 0.3 times the turnover rate (*65*).

Similar experiments in the back reaction of hexokinase have shown that glucose-6-*P* dissociates from E-glucose-6-*P* about 160 times faster than the enzyme turnover in the reverse reaction, and very slowly from E-glucose-6-*P*-MgADP (*66*).

In a preliminary report, Solheim and Fromm also have tried the isotope partitioning technique with MgATP in the forward reaction. They find that some of the initially bound radioactive ATP is converted to radioactive

product (*67*). This is excellent evidence that hexokinase can operate through a random mechanism.

8. *Conclusions*

When taken collectively, the overall evidence indicates that hexokinase can both add and release substrates and products in a random mechanism. However, the mechanism cannot be described as rapid equilibrium random. The evidence also indicates that the preferred pathway is the ordered addition of glucose followed by ATP, then the release of ADP followed by glucose-6-*P*. Danenberg and Cleland have recently attempted to assign relative rate constants to a general random mechanism for hexokinase as shown in Fig. 14 (*30*).

In this model the unimolecular constants are relative to the turnover number and the bimolecular constants are chosen to yield equilibrium constants in units of millimolar. The model is primarily based on dead-end inhibition by CrATP, the Michaelis constant for ATP in the ATPase reaction, the isotope partitioning experiments of Rose *et al.* (*65*), and various binding and kinetic constants found in the literature. The final model was based on a computer simulation study attempting to discover what combination of rate constants would fit the isotope partition data and the observed kinetic and binding constants.

This model predicts that 98% of the reaction flux will go through the pathway with glucose adding first when both glucose and MgATP are present at K_m levels. At higher MgATP levels both pathways would carry nearly equal flux (*30*).

E. X-Ray Structure

1. *Crystal Forms*

The x-ray structure determination of yeast hexokinase has been undertaken by the Steitz group at Yale University (*68*). Although the complete amino acid sequence of hexokinase has not been determined, much information about the structure and function of this enzyme has been determined from the x-ray picture presented thus far.

Work has progressed on three different crystal forms of hexokinase. These have been labeled BI, BII, and BIII. Form BI is in the space group $P2_1\ 22_1$ with 4 molecules per unit cell (*68*). An electron density map has been calculated to 6 Å resolution. The two subunits of hexokinase in this crystal form are related by a rotation of 180° plus a translation of 3.5 Å along the sym-

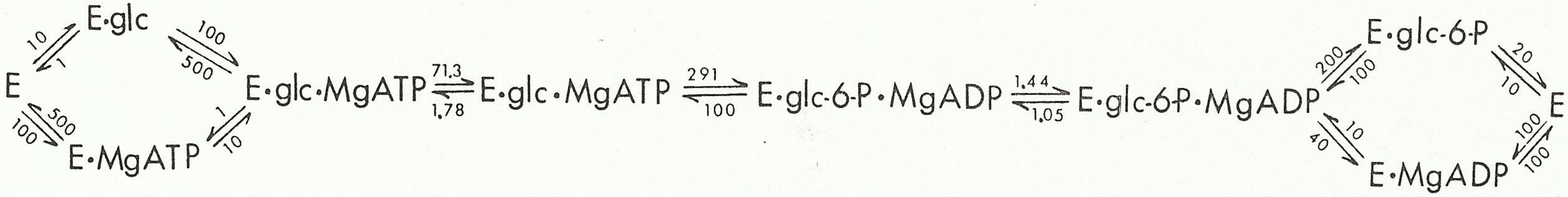

FIG. 14. Model for the kinetic mechanism of yeast hexokinase.

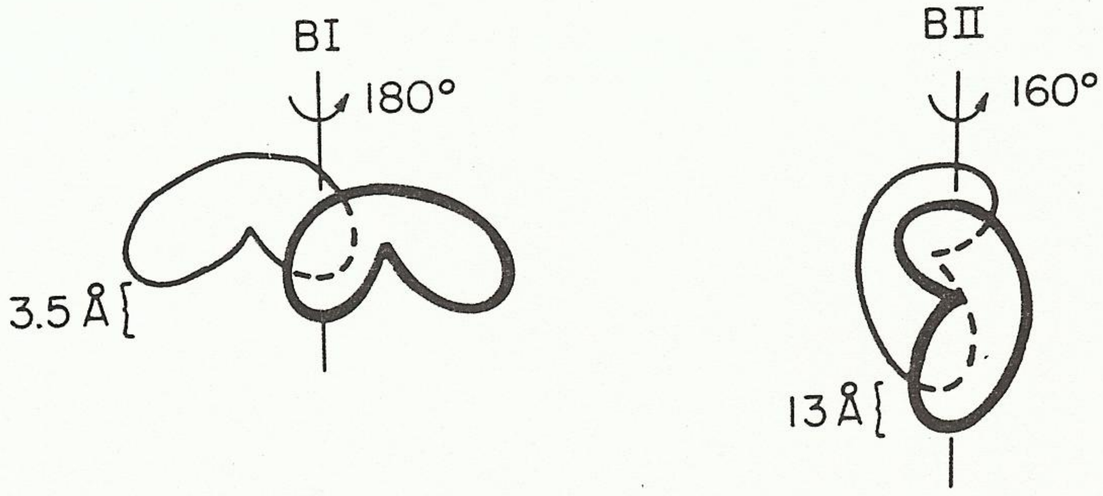

FIG. 15. A schematic drawing showing the difference in the arrangement of subunits found in the asymmetric unit of BI and BII crystals. From Anderson *et al.* (*70*).

metry axis (Fig. 15) (*69*). Each subunit appears to be identical and is bilobal with a narrow bridge of density between the lobes (*69*). The dimension of the dimer is 150 Å × 45 Å × 55 Å and each subunit is 80 Å × 40 Å × 50 Å (*69*). Unfortunately, neither glucose nor MgADP will bind to these crystals without disintegration of the protein crystals. This form has not been characterized further.

The BII crystals, grown in potassium phosphate, are also dimeric and will bind sugars and nucleotides (*70*). BIII hexokinase has been proteolytically modified. It is monomeric in solution and in the crystalline state (*71*).

2. *Quaternary and Tertiary Structure*

In the BII crystals the dimer has the overall dimensions of 90 Å × 85 Å × 60 Å. In addition, each subunit has the overall dimensions of 80 Å × 50 Å × 40 Å (*70*). Like the BI crystals, the two subunits in the BII crystals are not related by a simple 180° rotation axis. The subunits, however, are related by a 160° rotation axis coupled with a translation by 13 Å along the symmetry axis (Fig. 15) (*70*). The tertiary structure of the individual subunits in the BI and BII crystals appear to be identical.

Glucose and *O*-toluoylglucosamine bind to these crystals in the deep cleft that separates the lobes of each subunit (*70*). ADP or AMP–PNP only bind in the presence of a sugar substrate or inhibitor. Only one nucleotide binds per dimer, and its binding site is located at the point of contact between the two subunits (*72*). Parts of the binding site are on each subunit. This site has been labeled the I site (*72*). A schematic drawing of the BII structure with the location of the various binding sites is shown in Fig. 16 (*72*).

The third crystal form, BIII, contains one monomer per asymmetric unit and also binds glucose and AMP (*52*). Like the BII dimer, glucose binds in the deep cleft that separates the two lobes. AMP does not bind at the nucleotide site of the BII crystals since each monomer has only part of the complete

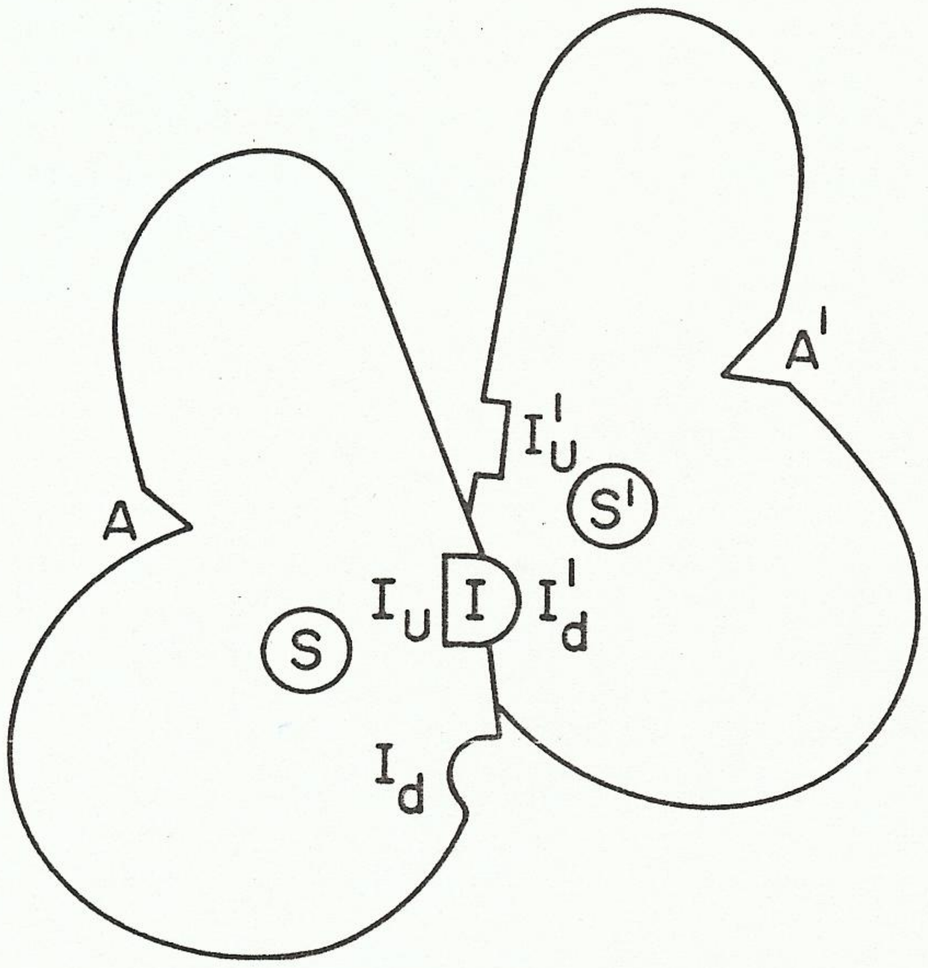

FIG. 16. A schematic drawing of the hexokinase dimer showing the location of observed glucose and nucleotide binding sites. The two sugar binding sites are represented by *S* and *S'*. The intersubunit AMP-PNP site I is formed by regions Iu and Id′ of each subunit. The symmetry related sites are indicated by Iu′ and Id. The location of the AMP binding sites in the monomeric BIII crystal form are labeled A and A′. From Anderson *et al.* (*72*).

site. AMP binds at another site close to the glucose site (*71*). This form has been determined to a 2.7 Å resolution. The tertiary structure of the BII is almost identical with the BII enzyme. A schematic drawing of the polypeptide backbone with the location of the various binding sites is shown in Fig. 17 (*71*).

3. *Intersubunit Site*

As mentioned, AMP-PNP or ADP in the presence of glucose will bind only to the BII crystals at a site between the two subunits. Nucleotides bound at this site appear to be in a fully extended conformation (*73*). ATP analogs bound at this site make contact with amino acid residues from both subunits. The γ-phosphate of ATP bound at this site is 20 Å from the 6-hydroxyl of bound glucose on one subunit and 30 Å from the glucose on the other subunit (*73*). It has been proposed that this site is an allosteric regulatory site for hexokinase and not the substrate site for ATP where phosphoryl transfer occurs (*73*).

4. *ATP Site*

The intersubunit site does not exist in the monomeric BIII crystals. AMP binds to these crystals at another site labeled the "A site." Model building,

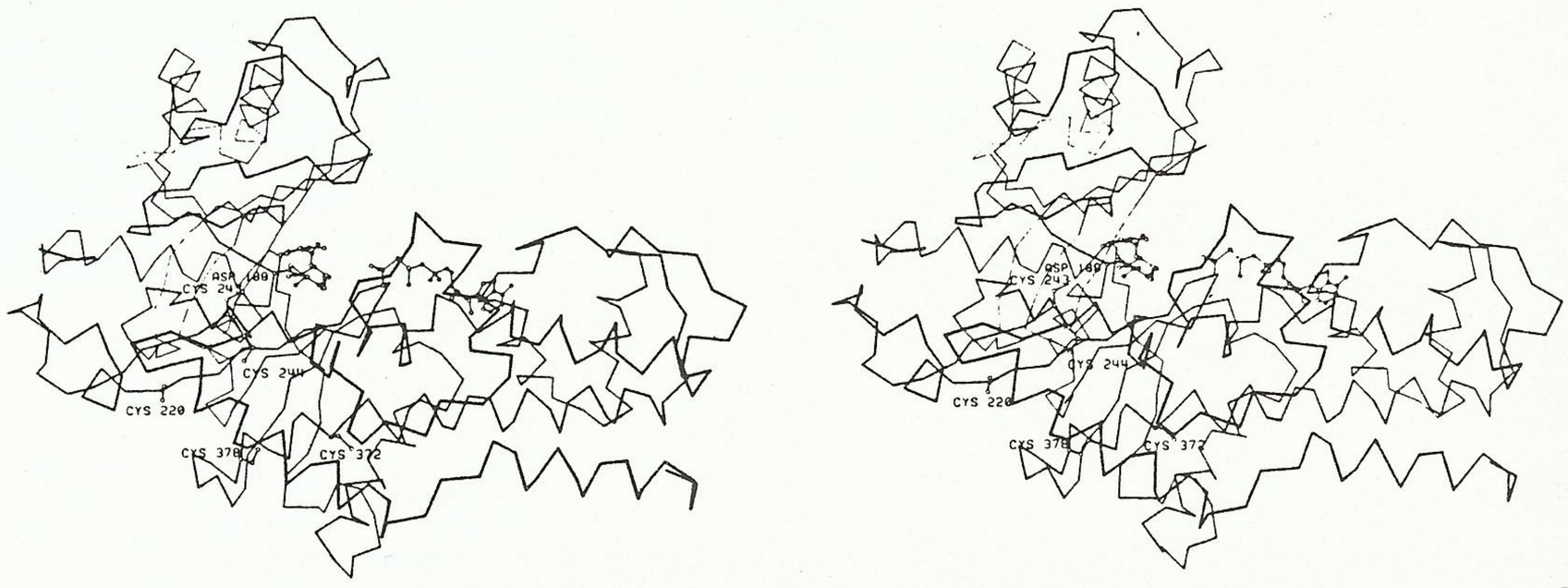

FIG. 17. A schematic drawing of the course of the polypeptide backbone of yeast hexokinase. From Anderson *et al.* (*74*). Reprinted with permission of Academic Press.

based on AMP and sulfate difference maps, with ATP at this site show it to be in an extended conformation (*73*). When placed in this manner, the γ-phosphate of the ATP is only 6 Å from the 6-hydroxyl of the bound glucose molecule. It has therefore been proposed that this be the active site for ATP (*73*).

5. *Glucose Site*

Glucose binds in both the BII and BIII crystal forms in the deep cleft separating the two lobes of each subunit. Glucose appears to bind in the C-1 (chair equatorial) α-D-glucopyranose conformation (*73*). All of the hydroxyls, except the 1-hydroxyl, are thus in an equatorial position. Protein side chains are hydrogen bonded to the 3-, 4-, and 6-hydroxyls and possibly to the 1-hydroxyl of glucose. The 2-hydroxyl appears to be pointing toward open space (*73*). This corresponds nicely with the observed substrate specificity.

Although the amino acid sequence is not known, the specific amino acid residues at the active site of hexokinase have been attempted to be determined through a crystallographic refinement of the data to 2.1 Å (*74*, *75*). Steitz and co-workers have concluded that Asp-189 is hydrogen bonded both to the 6- and 4-hydroxyl groups of glucose. The 4-hydroxyl is also hydrogen bonded to Asx-188 and Asx-215. The 3-hydroxyl interacts with Asx-245 and Asx-188 (*76*). The appearance of an aspartic acid residue at the active site hydrogen bonded to the 6-hydroxyl is consistent with recent kinetic evidence.

F. CHEMICAL MECHANISM

From pH kinetic studies, Viola and Cleland have proposed that hexokinase requires a group on the enzyme that must be unprotonated for the forward

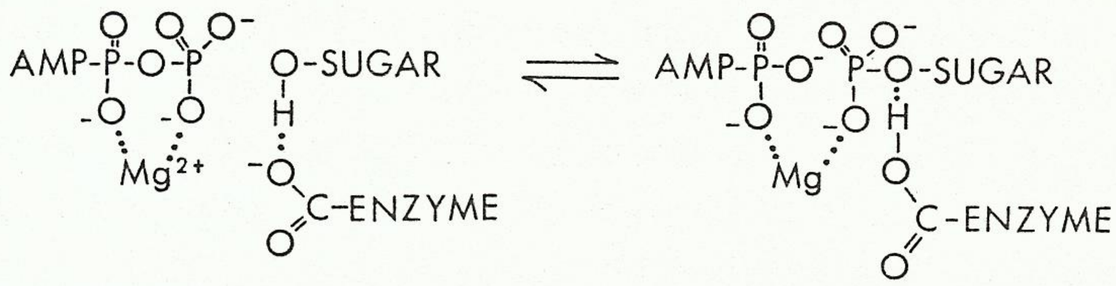

FIG. 18. A schematic drawing of the chemical mechanism of yeast hexokinase.

reaction and protonated for the reverse reaction (*77*). This group has been identified as a carboxylic acid from its enthalpy of ionization and behavior in organic solvents (*77*). In agreement with this are results from chemical modification studies which show that all of the histidine groups can be modified without complete loss of activity (*78*). Steitz *et al.* have also shown that there appears to be an aspartic acid residue hydrogen bonded to the 6-hydroxyl of glucose in the x-ray picture of hexokinase (*76*). The pH kinetic studies and the x-ray data suggest that during catalysis this carboxyl is acting as a general base in accepting a proton from the glucose in the forward reaction, and acting as a general acid in the back reaction by donating a proton to glucose-6-*P*. This would tend to increase the nucleophilicity of the 6-hydroxyl and facilitate its attack on the γ-phosphoryl of ATP (*76*). This is shown schematically in Fig. 18.

G. CONCLUSIONS

The role of the metal ion in hexokinase seems to be to coordinate the β,γ phosphate groups of ATP. In this manner the metal ion serves as an electrophilic center to neutralize the negative charges on the ionized phosphate groups of ATP. This then leads to facilitated catalytic attack by the 6-hydroxyl group of substrate on the γ-phosphoryl of ATP.

IV. Glutamine Synthetase

A. BACKGROUND

The reaction that glutamine synthetase catalyzes is the following:

$$\text{L-glutamate} + \text{ATP} + \text{NH}_3 \overset{2M^{2+}}{\rightleftharpoons} \text{L-glutamine} + \text{ADP} + \text{P}_i$$

Divalent cations are required for activity (Mg^{2+}, Mn^{2+}, Co^{2+}) regardless of the origin of the enzyme. The role of these metal ions in catalysis, as well as regulation of catalysis, has been the subject of numerous reviews (*79–84*).

Homogeneous preparations of glutamine synthetase are available from many sources including *Escherichia coli*, *Salmonella typhimurium*, peas, sheep brain, and rat liver. Glutamine synthetases from bacteria have 12

subunits, while the enzymes from mammals have eight. The subunit sizes of all glutamine synthetases are 44,000–50,000.

Glutamine synthetase has a central role in nitrogen metabolism and presently there is substantial interest in all aspects of catalysis and regulation of this key enzyme. The synthesis of glutamine is probably the most central reaction in nitrogen metabolism. The amide nitrogen of glutamine is involved in production of amino acids for protein biosynthesis and DNA biosynthesis, as well as other important metabolic compounds (including several enzyme cofactors). The regulation of glutamine synthetase activity in *E. coli* has been reviewed (*79, 81–83*). Glutamine is an important intermediate in the assimilation of ammonia by *E. coli* and, consequently, a rigorous cellular control has evolved. The synthesis of the enzyme is decreased when *E. coli* are grown on media high in ammonia, whereas growth conditions on limiting ammonia produce a 20-fold increase of the enzyme. Additionally, feedback inhibition by multiple end products of glutamine metabolism (L-alanine, glycine, L-histidine, L-tryptophan, cytidine triphosphate, adenosine monophosphate, glucosamine-6-*P*) also regulate the activity of existing glutamine synthetase molecules. The enzyme presumably contains separate sites for each of the above-mentioned inhibitors. The main emphasis of this section is to summarize the kinetics, NMR, and EPR work with the enzyme and to speculate on the role of the metal ions in catalysis.

Escherichia coli have also developed an elegant method to control enzyme catalysis that occurs by covalent modification of each subunit. In this latter reaction a single tyrosyl residue per subunit is adenylylated to produce a stable 5′-adenylyl-*O*-tyrosyl derivative. Recent NMR and fluorescence data will be reviewed concerning the nature of this adenylyl site and its spatial relationship to the metal ions at the catalytic site. The enzymes responsible for the covalent adenylylation reaction comprise a "cascade system" for amplifying the activation or inactivation of glutamine synthetase molecules (*81*).

Experimental techniques for determining distances must be employed to establish the structure of the active site components of glutamine synthetase. Techniques that are available for these studies are x-ray crystallography, EPR, NMR, and fluorescence energy transfer. All approaches are currently being employed to study the structure and function of this metalloenzyme.

B. Kinetic Mechanism

Since the reaction catalyzed by glutamine synthetase has three substrates (L-glutamate, NH_3, and metal-ATP) and three products (L-glutamine, P_i, and metal-ADP), the kinetic mechanism as deduced by steady-state kinetics

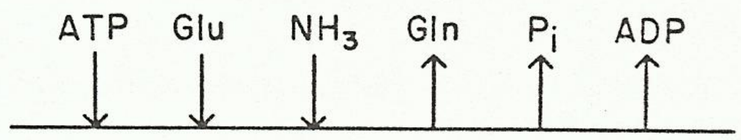

Scheme I

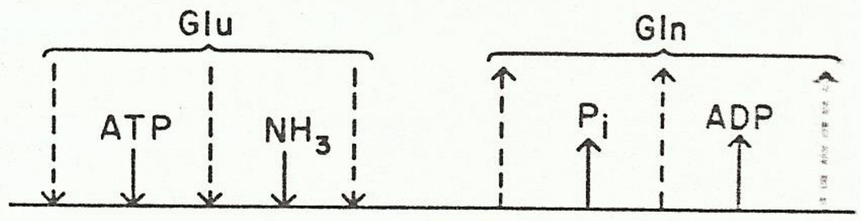

Scheme II

FIG. 19. Two proposed kinetic schemes for the glutamine synthetase reaction.

presents a challenging problem. To simplify the situation we will consider only two alternative mechanisms (Fig. 19) and review the supporting or refuting data.

One mechanism involves the sequential ordered addition of ATP (this is always metal–ATP), L-glutamate, and ammonia prior to release of any products. Another mechanism has a random (but sequential) order of addition of all substrates, and perhaps a random order of product release.

The dashed lines indicate L-Glu binding at any of the three points in the sequence. For a completely random addition of substrates, the positions of binding of ATP and NH_3 could also be reversed.

1. *Isotope Exchange at Equilibrium*

The kinetic approach that has been most extensively applied to glutamine synthetase is that of equilibrium isotope exchange (*85–88*). Experimental procedures involve preparing a series of reaction solutions at chemical equilibrium and monitoring the following exchanges:

$$[^{14}C]\text{glutamate} \rightleftharpoons [^{14}C]\text{glutamine}$$

$$[^{15}N]NH_3 \rightleftharpoons [^{15}N]\text{glutamine}$$

$$[^{32}P]P_i \rightleftharpoons [^{32}P]ATP$$

$$[^{14}C]ADP \rightleftharpoons [^{14}C]ATP$$

Scheme I

Results of such experiments with enzymes from the sheep brain, pea seed, and *E. coli* (*87*) show that, without exception, the relative rates of exchange are (glutamate ⇄ glutamine) > (NH_3 ⇄ glutamine) > (P_i = ATP) ≃ (ADP ⇄ ATP). If the substrate interconversion were the rate-limiting step

in catalysis all exchanges would be equal at equilibrium. Since this is not the case and since ADP ⇄ ATP is the slowest exchange rate, the overall rate of the enzymic reaction is limited (partially at least) by nucleotide release. However, a distinction in mechanisms exists for the sheep brain enzyme as contrasted with the enzyme from the pea seed and *E. coli*. The latter two enzymes exhibit kinetic isotope exchange patterns consistent with random substrate addition and release (but still catalysis is limited by nucleotide release), whereas the enzyme from sheep brain has a preferred order of addition of substrates consistent with the preceding scheme I.

2. *Isotope Exchange During Net Enzymatic Reaction*

Recent experiments with $[^{18}O]P_i$ and *E. coli* enzyme by Stokes and Boyer (*89*) and Balakrishnan *et al.* (*90*) show that transfer of oxygens from P_i to glutamine is the most rapid of the measured isotopic exchanges. The reaction for net formation of ATP follows.

$$[^{18}O]P_i + ADP + \text{L-Gln} \rightarrow \text{L-Glu} + NH_3 + ATP$$

The partial reaction of the ^{18}O exchange from $[^{18}O]P_i$ to L-glutamine was 5–7 times faster than net ATP formation. This establishes (along with the equilibrium isotope exchange data) the following order of events with the *E. coli* enzyme.

$$\text{ATP release} < NH_3 \text{ release} < \text{L-glu release} < \text{substrate interconversion} <$$

$$\text{L-gln release} \leq P_i \text{ release} < \text{ADP release}$$

Stokes and Boyer also conclude that the carboxyl of bound glutamate must be free to rotate to produce the observed ^{18}O exchange from $[^{18}O]P_i$ to L-glutamine.

The experiments of Balakrishnan *et al.* (*90*) utilized an NMR approach developed by Cohn and Hu (*91*) that permitted following the change in isotopic distribution during the reaction of the P_i species $P[^{18}O]_4$, $P[^{18}O]_3[^{16}O]_1$, $P[^{18}O]_2[^{16}O]_2$, $P[^{18}O]_1[^{16}O]_3$, and $P[^{16}O]_4$. This technique relies on differences in chemical shift owing to the number of ^{18}O and ^{16}O isotopes in P_i (Fig. 20). The rate constant for $^{16}O/^{18}O$ exchange was 410 ± 40 min^{-1} compared to 62 ± 4 min^{-1} for net ATP synthesis. Figure 21 shows the change in species composition with time.

Two other points that arise from these data are that the change in isotopic distribution in P_i follows a binomial distribution throughout the exchange reaction, which means that P_i is rapidly rotating on the enzyme surface and that only one oxygen of P_i is exchanged with ^{16}O of glutamine per catalytic encounter. These conclusions necessitate that P_i release > L-glutamine

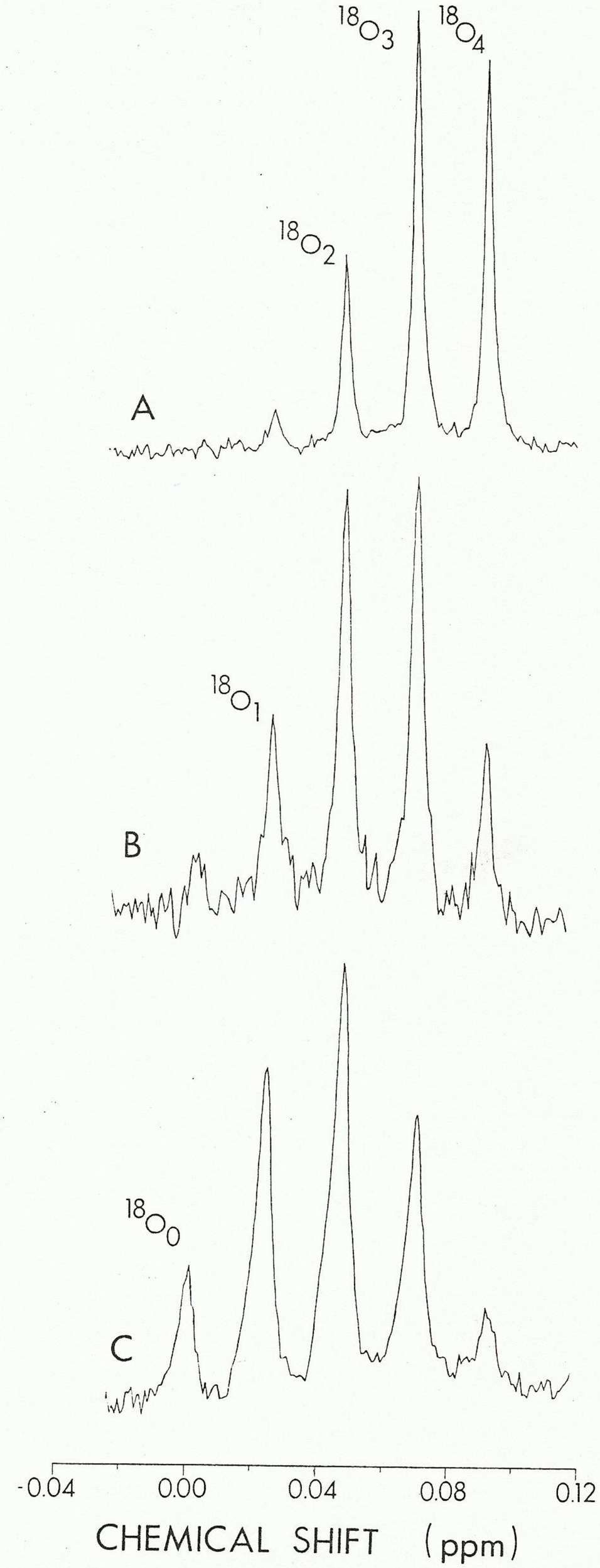

FIG. 20. ^{31}P nuclear magnetic resonance spectra of ^{18}O-enriched inorganic phosphate. $[^{18}O]_4$, $[^{18}O]_3$, $[^{18}O]_2$, $[^{18}O]_1$, and $[^{18}O]_0$ refer to $P[^{18}O]_4$, $P[^{18}O]_3[^{16}O]_1$, $P[^{18}O]_2[^{16}O]_2$, $P[^{18}O]_1[^{16}O]_3$, and $[^{16}O]_4$, respectively. Taken from Balakrishnan *et al.* (*90*) with permission of Academic Press.

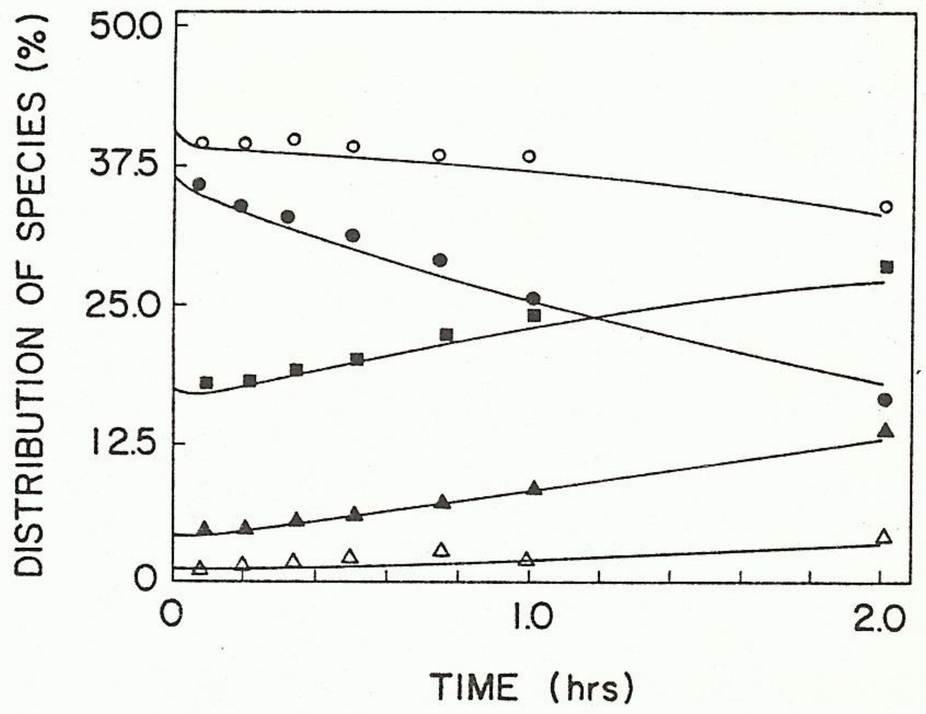

FIG. 21. Time-course for phosphate–oxygen exchange catalyzed by glutamine synthetase. The fractional concentrations of the species $P[^{18}O]_4$ (●), $P[^{18}O]_3[^{16}O]_1$ (○), $P[^{18}O]_2[^{16}O]_2$ (■), $P[^{18}O]_1[^{16}O]_3$ (▲), and $P[^{16}O]_4$ (△) are plotted vs. time for the scheme given in Balakrishnan *et al.* (*90*). Reprinted with permission of Academic Press.

release. With other systems, e.g., myosin (*92*) and inorganic pyrophosphatase (*93*), more than one oxygen of P_i is exchanged with H_2O on the enzyme before P_i departs. Figure 22 depicts the probable catalytic events with glutamine synthetase.

3. *Initial Velocity Studies*

Recent steady-state kinetic data from this laboratory suggest that the *E. coli* enzyme can operate under certain conditions by a preferred ordered pathway (scheme I). Parallel initial velocity patterns are predicted for scheme I of plots of 1/velocity vs. $1/[NH_4^+]$ at varying concentrations of ATP and saturating L-glutamate. However, at subsaturating levels of L-glutamate the patterns should intersect. This has been found experimentally. These data suggest that under initial velocity conditions the enzyme may function by a preferred pathway, but under equilibrium conditions the data conform to a random pathway. The fluorescence data of Timmons *et al.* (*94*) demonstrate that ATP or L-glutamate can bind independently, but prior binding of ATP tightens the binding constant for L-glutamate from ~20 m*M* to ~3 m*M*. This is termed substrate synergism, and may lead to a preferred pathway for catalysis reflected in the initial velocity experiments. It may be recalled that the kinetic data for hexokinase also gave conflicting results with regard to the kinetic order of substrate binding.

Midlefort and Rose (*95*) used an isotope scrambling method to detect the rapid and reversible formation of a γ-glutamyl phosphate adduct on the

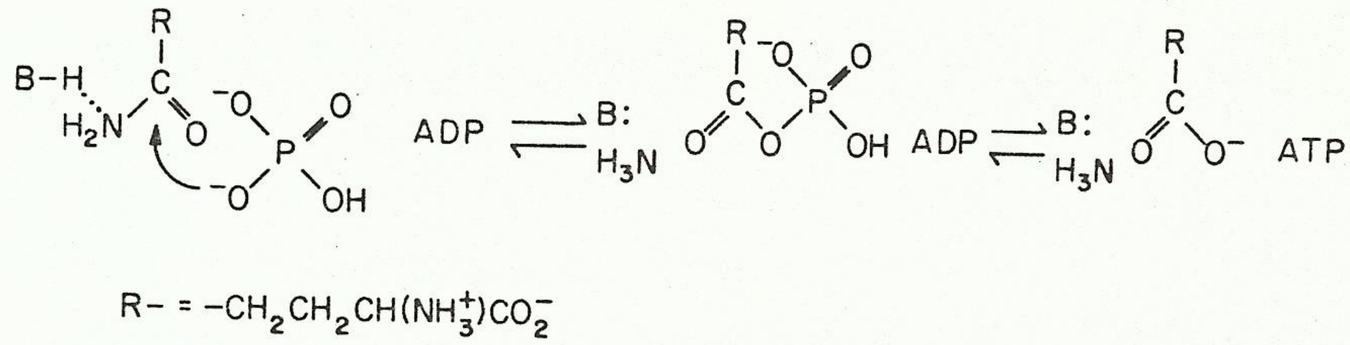

FIG. 22. Proposed catalytic sequence of reactions catalyzed by glutamine synthetase.

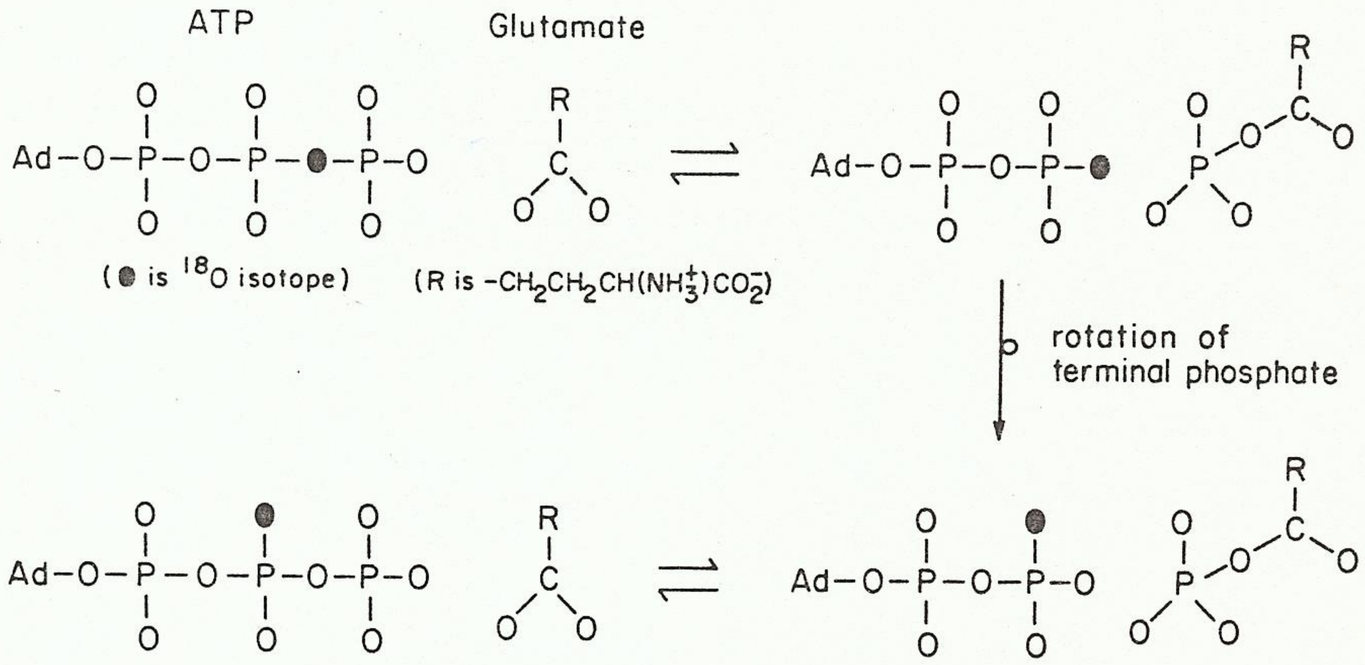

FIG. 23. Scheme showing the scrambling of ^{18}O label in ATP catalyzed by glutamine synthetase.

enzyme from glutamate and ATP. Their method, as depicted in Fig. 23, is consistent with an ordered pathway (scheme I) and with the data summarized by Meister (*80*) pertaining to the existence of γ-glutamyl phosphate as an intermediate in the enzymic mechanism (see the following section).

These experiments were conducted with sheep brain and *E. coli* enzymes, and for both enzymes a minimum two-step mechanism was proposed where phosphoryl transfer precedes the chemical reaction with the third substrate ammonia.

C. Analogs of the Transition State or Intermediates in the Reaction

Many years ago Meister's group (*96–101*) synthesized of a number of inhibitors or substrate analogs that would mimic the intermediates in the proposed pathway of the reactions catalyzed by glutamine synthetase. Two of these are listed below, along with the structures for substrates and two alleged intermediates.

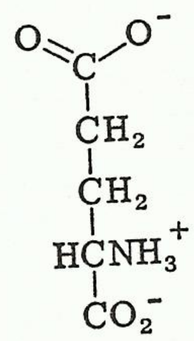

L-Glutamate

I

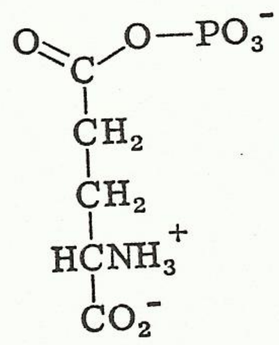

γ-Glutamyl phosphate

II

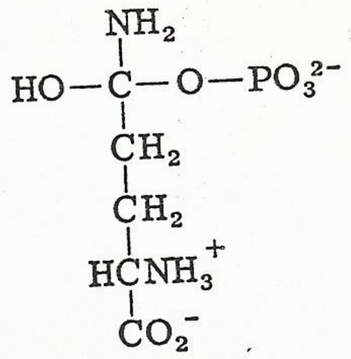

Tetrahedral adduct

III

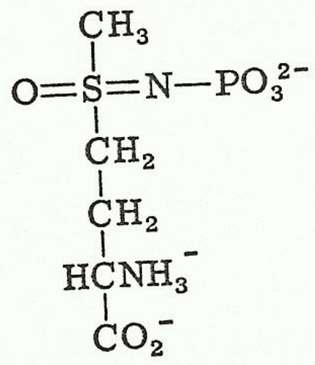

L-Methionine-(S)-sulfoximine phosphate

IV

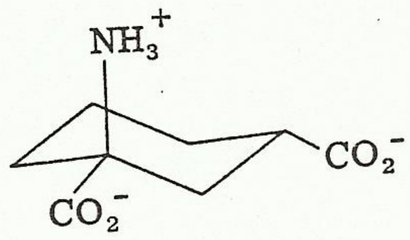

cis-1-Amino-1,3-discarboxycyclohexane

V

Gass and Meister found that the *cis*, but not the *trans* isomer of 1-amino-1,3-dicarboxycyclohexane (V), was a substrate analog of L-glutamate (I). Fifty percent of the *DL* mixture of compound V reacted as a substrate, which leads to the conclusion that the extended form of L-glutamate was bound to the enzyme during catalysis. Other data of Khedouri *et al.* (*100*) on β-amino glutamyl phosphate and the acyl phosphate derivatives of compound V (*101*) demonstrate that these substrate analogs can participate in the enzymic reaction and lend credence to the formation of γ-glutamyl phosphate (II) during the reaction mechanism. The kinetic consequences of the formation of γ-glutamyl phosphate are, however, unclear. Equilibrium isotope data (*87*) are consistent with the formation of γ-glutamyl phosphate with the sheep brain enzyme, but are equivocal for its "long-life" during catalysis with the *E. coli* enzyme.

The above data, along with other data from Meister's group (*102*, *103*), provided the basis for computer modeling studies (*104*) of the active site conformations of substrates and intermediates in the glutamine synthetase reaction. The conclusions are that both structures II and III are in the reaction mechanism.

Rowe *et al.* (*97*) found that glutamine synthetase was irreversibly inhibited by methionine sulfoximine in the presence of ATP. Also, they discovered

that the enzyme catalyzed the formation of methionine sulfoximine phosphate. The tight complex of ADP and methionine sulfoximine phosphate with the enzyme is apparently responsible for the irreversible inhibition. Manning *et al.* (*98*) found that L-methionine-(*S*)-sulfoximine (IV) was the diastereomer that inhibited glutamine synthetase under their experimental conditions. Later kinetic data by Wedler and Horn (*87*) demonstrated that methionine sulfoximine was a competitive inhibitor vs. glutamate with a dissociation constant of 1.5 μM. This value represents three orders of magnitude tighter binding of the inhibitor when compared to glutamate binding (K_D = 3 mM). This is the expected behavior for a compound that is a transition-state analog (*105*). The tetrahedral configuration of atoms at the sulfur of methionine sulfoximine would mimic the tetrahedral adduct (III) proposed along the reaction pathway. In a recent report, NMR and EPR data from this laboratory concerning the involvement of Mn(II) in the reaction mechanism were reported. These data support the hypothesis of tetrahedral adduct formation in the reaction mechanism. This will be discussed in the following section.

Another interesting point explored in detail by Wedler and Horn (*87*) is that the "apparent binding constant" of methionine sulfoximine for the irreversible inhibition is $\sim$100 μM compared to 1.5 μM for direct binding to the enzyme. This leads to speculation that perhaps methionine sulfoximine can bind to the enzyme in two conformations; one for competitive binding that does not lead to irreversible inhibition, while another conformer binds in a different manner, producing the irreversible inhibition. The proposal from computer modeling studies of Gass and Meister (*104*) is that one conformation is responsible for both, but recent data open the door for further study and speculation.

Four other compounds have been tested as inhibitors of glutamine synthetase.

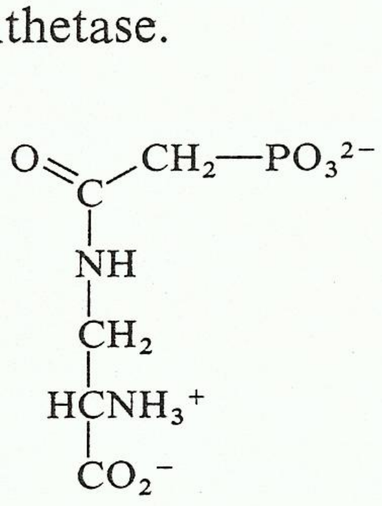

VI

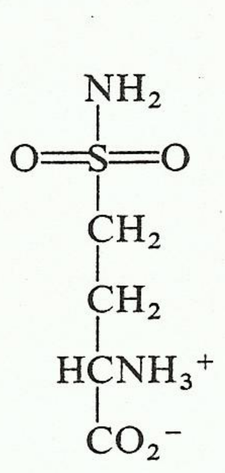

VII

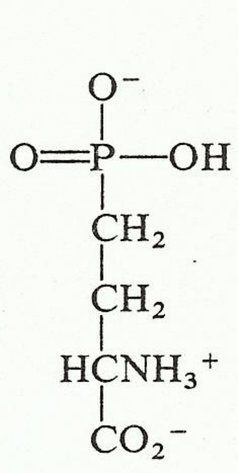

VIII

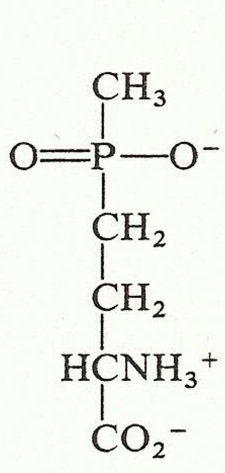

IX

Compound VI was found by Wedler and Horn to be a weak competitive inhibitor of the enzyme with a dissociation constant of $\sim$3 mM. This compound should mimic the γ-glutamyl phosphate intermediate (II). From this

initial study it appears that this compound does not bind to the enzyme as tightly as one would expect for a transition-state analog.

The newly synthesized inhibitor (VII) was studied by Meek and Villafranca (*106*). Compounds VII (*106*) and VIII (*107*) have the tetrahedral atoms sulfur and phosphorus at the critical tetrahedral location, and were found to be good competitive inhibitors of the enzymic reaction having binding constants of $\sim 4.5 \times 10^{-5}$ M. Compound IX (*108*) has a binding constant of 7×10^{-6} M. Thus extensive data on substrate analogs and intermediate analogs lead to the conclusion that the enzyme stabilizes binding of an adduct of the type depicted in structure III, but does not especially stabilize binding of a planar adduct at the stage in the reaction of γ-glutamyl phosphate (II).

D. EPR and NMR Studies of Conformational Changes at the n_1 Metal Ion Site

As discussed earlier, the enzymic reaction catalyzed by glutamine synthetase requires the presence of divalent metal ions. Extensive work has been conducted on the binding of Mn^{2+} to the enzyme isolated from *E. coli* (*82*, *109–112*). Three types of sites, each with different affinities for Mn^{2+}, exist per dodecamer: n_1 (12 sites, 1 per subunit) of high affinity, responsible for inducing a change from a relaxed metal ion free protein to a conformationally tightened catalytically active protein; n_2 (12 sites) of moderate affinity, involved in active site activation via a metal–ATP complex; and n_3 (48 sites) of low affinity unnecessary for catalysis, but perhaps involved in overall enzyme stability. The state of adenylylation and pH value alter the metal ion specificity and affinities.

1. *Binding Constants*

Adenylylated subunits bind Mn^{2+} tightly, resulting in a catalytically active enzyme, whereas an unadenylylated enzyme is specifically activated for catalysis by Mg^{2+}. Unadenylylated enzyme binds Mn^{2+} with about equal affinity as the fully adenylylated enzyme ($K_1 = 5 \times 10^{-7}$ M) at the n_1 sites. The affinity of Mn^{2+} for the n_2 sites is about two orders of magnitude weaker than that for the n_1 sites, but the presence of glutamine tightens the Mn^{2+} binding at n_2 to about 5×10^{-7} M for the fully adenylylated enzyme (*112*). Thus, even though multiple metal ion sites are involved, careful experimental design can produce meaningful results in delineating the role of the two catalytically important metal ion sites. Indeed, our NMR and EPR results show that the "tight" metal ion site is likely involved in orienting the γ-carboxylate of glutamate, and the second metal ion site (metal–ATP site) is close to the tight n_1 site.

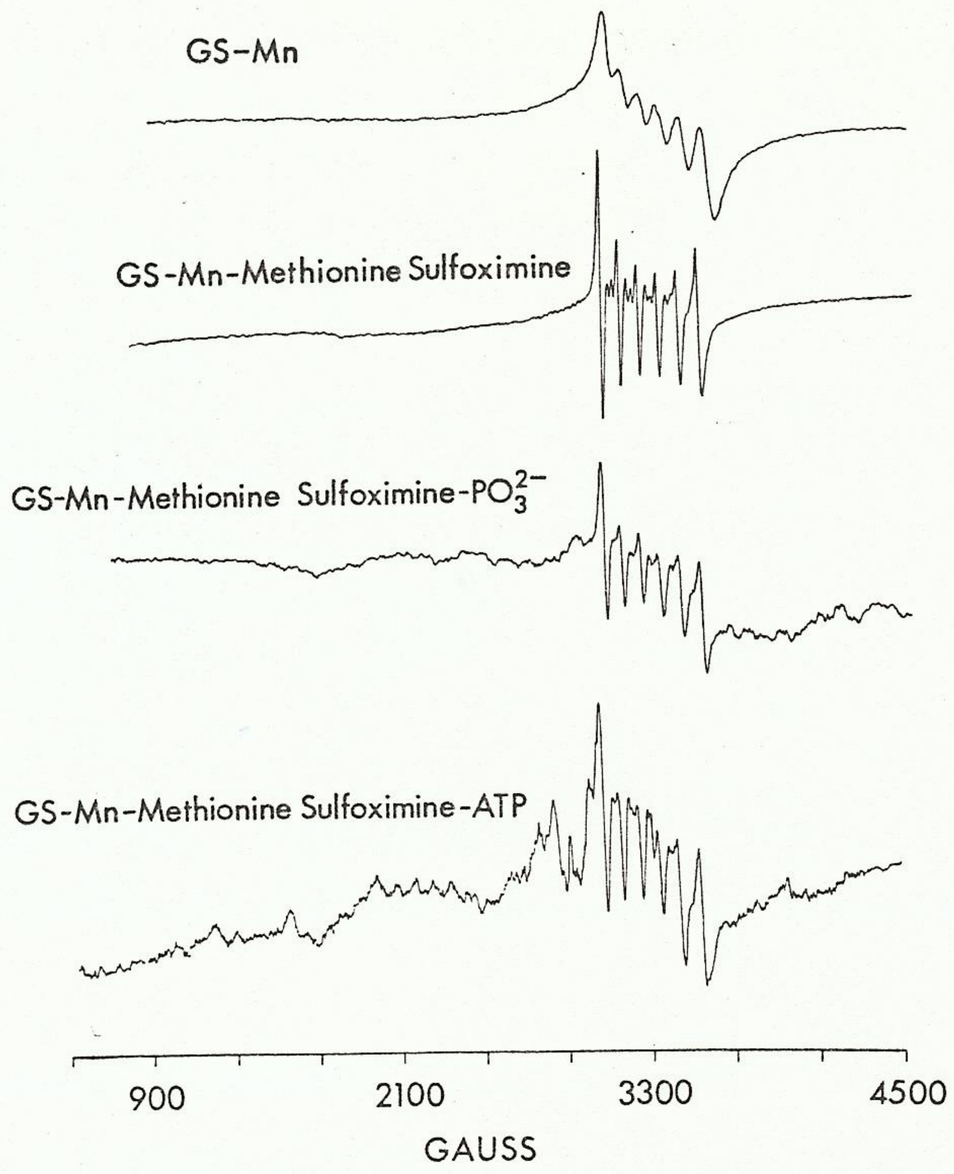

FIG. 24. EPR spectra at *x*-band for some complexes of glutamine synthetase. Reprinted with permission of the American Chemical Society from Villafranca *et al.* (*113*).

Since the binding constants of Mn^{2+} to the tight and weak metal ion sites of unadenylylated enzyme are 5.0×10^{-7} and 4.5×10^{-5} *M*, respectively, the tight site can be selectively populated under conditions where [enzyme] > [Mn^{2+}]. Figure 24 shows EPR spectra obtained with a solution of 0.79 m*M* enzyme subunit concentration and 0.7 m*M* Mn^{2+} concentration (*113*). This spectrum represents Mn^{2+} bound only at the tight sites with no free Mn^{2+} present. It shows that bound Mn^{2+} is in a relatively isotropic environment (i.e., the zero-field splitting is small).

2. *Effects of Substrates and Analogs*

Our studies of the substrates [glutamate (I) and ATP] and of substrate analogs [AMP-*P*-(CH_2)-*P* and methionine sulfoximine] reveal interactions between both substrate sites and both metal ion sites. Previously mentioned studies by Meister's group showed that the irreversible inhibition of glutamine synthetase in the presence of L-methionine (S)-sulfoximine and ATP was due to formation of the sulfoximine phosphate (IV). The tetrahedral geometry at the sulfur atom of the sulfoximine was suggested to be a "mimic" of the "active structure" of the adduct of γ-glutamyl phosphate and ammonia (III). Data in our laboratory provide spectroscopic evidence that methionine

sulfoximine and the sulfoximine phosphate are transition-state analogs of the glutamine synthetase reaction (*113–115*).

In the presence of a saturating concentration of L-methionine (SR)-sulfoximine, a dramatic change in the line width and resolution of the EPR spectral intensities of Mn^{2+} bound at n_1 are noted. The line widths change from about 30 G peak to peak, to about 12 G (middle spectrum, Fig. 24). Two observations can be made about this spectrum: (1) the narrow line widths are symptomatic of Mn^{2+} ions that are occluded from solvent bombardment and this is supported by NMR data of solvent water relaxation in enzyme solutions containing saturating concentrations of L-methionine (SR)-sulfoximine; (2) the bound Mn^{2+} is in a nearly cubic environment based on the EPR spectrum that shows six $-\frac{1}{2}$ to $\frac{1}{2}$ transitions centered near $g = 2$ with resolved forbidden transitions and no apparent transitions at higher or lower field strengths. Thus L-methionine (SR)-sulfoximine may have induced a distortion of the metal ion environment as a result of a displacement of solvent. Alternatively, close proximity of sulfoximine to the Mn^{2+} ion (~5 Å) may have immobilized a water molecule in the coordination sphere producing the observed distortion of the Mn^{2+} ion.

When 3.3 m*M* L-methionine (SR)-sulfoximine phosphate is present in a solution of enzyme-Mn^{2+}, the resultant spectrum is quite different from that detected for the unphosphorylated sulfoximine. Additional fine structure splittings are noted around 3300 G, in addition to poorly resolved resonances at about 2400 G. This indicates that the sulfoximine phosphate binds to the enzyme differently and induces different changes in the Mn^{2+} spectra than either the sulfoximine itself or the methionine sulfoximine phosphate formed *in situ*. The addition of 10 m*M* $MgCl_2$ and 10 m*M* ADP to an enzyme solution containing the sulfoximine phosphate did not produce significant spectral changes from those shown in Fig. 24.

The spectrum at the bottom of Fig. 24 is obtained when MgATP is added to a solution of enzyme-Mn^{2+}-L-methionine (SR)-sulfoximine. The solution is allowed to incubate for 10 min at 25°C, cooled to 1°C, and then the spectrum is taken. This spectrum is quite reproducible if Mg^{2+} and ATP are added in a 1:1 ratio at a two- to five-fold molar excess over enzyme. Higher concentrations produced no additional changes. No detectable changes are seen in the spectrum of enzyme–Mn^{2+}–L-methionine (SR)-sulfoximine with a 40-fold excess of either Mg^{2+} or ATP alone. This experiment demonstrates that Mn^{2+} is locked into the tight metal ion site by the sulfoximine and not displaced or perturbed by Mg^{2+} or ATP alone. Thus, the presence of MgATP produces a dramatic change in the spectrum of bound Mn^{2+} when this complex is bound at the metal ion–nucleotide site. This spectrum could result from the *in situ* formation of the sulfoximine phosphate and result in stabilization of an enzyme conformation and Mn^{2+}

distortion unobtainable with the separate addition of sulfoximine phosphate and ADP.

3. *NMR Studies*

Analysis of NMR titration data with sulfoximine in the presence of ATP gave a dissociation constant of 0.8 μM (*113*). The K_I value from kinetic determinations of Wedler and Horn (*87*) for L-methionine (SR)-sulfoximine is 1.5 μM with inhibition being linearly competitive with respect to L-glutamate. These kinetic and spectroscopic approaches provide the first direct measurement of the equilibrium binding constant for L-methionine (SR)-sulfoximine to the Mn enzyme. Interestingly, the conversion of the γ atom from trigonal (carbon for glutamate) to tetrahedral (sulfur for sulfoximine) symmetry results in a decrease in the binding constant by two orders of magnitude (from 3 mM to 30 μM), comparing L-glutamate to the L-sulfoximine. The binding of ADP and P_i to the sulfoximine–enzyme complex tightens the binding approximately another tenfold, whereas the phosphorylation of the inhibitor by ATP lowers the binding constant by only about fivefold. This suggests that the tight binding of the sulfoximine is primarily due to tetrahedral geometry at the γ position and conformational effects (synergism of binding) by bound nucleotide rather than to formation of a phosphorylated intermediate.

Other published EPR data show that L-glutamate produces a small axial distortion on the environment of enzyme–Mn(II) with unresolved fine structure and no obvious change in line width. Addition of MgATP results in a diminution of all spectral intensities and the anisotropic spectrum shows poorly resolved fine structure splitting. The appearance of these additional sets of transitions indicates that the environment of Mn^{2+} at the tight site is changed when metal nucleotide is bound. NH_4^+ produces additional subtle changes in the EPR spectrum of Mn^{2+}.

The EPR data presented provide a model of the active site in which Mn^{2+} at the tight n_1 metal ion site may be involved in orienting the substrate L-glutamate and substrate analog inhibitors. This orientation in the metal ion site is influenced by the addition of the substrates MgATP and NH_4^+ since progressive changes in the EPR spectra are observed. Also, the tetrahedral geometry of the sulfoximine may represent a transition state structure for the enzymic reaction.

E. Metal–Metal Distances between the n_1 and n_2 Sites

Recent data from this laboratory (*115*, *116*) gave the first distance determinations between the two metal ion sites of glutamine synthetase. In these

experiments, the interaction between two enzyme-bound paramagnetic metal ions was monitored by EPR and the results were used for calculations of metal–metal distances employing the Leigh theory (*117*). The procedure involved binding of Mn^{2+} at one site and Cr^{3+}-ATP, Cr^{3+}-ADP, or Co^{2+}-nucleotides at the metal–nucleotide site. These studies represented the first estimates of metal–metal distances on an enzyme by this EPR technique.

Briefly, Leigh's theory considers how the rigid lattice line shape of an EPR signal (Mn^{2+} at n_1) is influenced by a dipolar interaction of a second rigid spin (e.g., Cr^{3+}). When the dipolar interaction is dominated by a correlation time, τ, that is short with respect to the rotation of the macromolecule (the rigid lattice into which the two spins are "imbedded"), the result is not an observed broadening of the EPR signal, but instead only an "apparent" diminution in spectral amplitude. The decrease in signal can be used to calculate metal–metal distances.

First it was established by kinetic methods that the substitution-inert Cr^{3+}-nucleotides, CrADP and CrATP, were inhibitors of unadenylylated *E. coli* glutamine synthetase. Both complexes were linear competitive inhibitors versus MgATP in the biosynthetic assay. The K_I values were 9.6 $\pm$ 0.6 μM and 25 $\pm$ 1 μM for CrATP and CrADP, respectively. Addition of a saturating amount of CrATP produces a 60% decrease in the EPR spectrum of enzyme-bound Mn^{2+}. This electronic spin–spin interaction between Mn^{2+} and Cr^{3+} was analyzed at both 9 and 35 GHz. A distance of 7.1 Å between Mn and Cr was obtained by analysis of these EPR data using the Leigh theory. Titration experiments with CrATP were conducted by following the decrease in the EPR spectral amplitude of enzyme–Mn^{2+}, and a K_D value of 0.30 $\pm$ 0.04 mM was calculated. The above experiments were also conducted in the presence of glutamate, glutamine, or methionine sulfoximine (see Fig. 25). The K_D and metal–metal distances were 0.28 mM and 5.2 Å, 0.055 mM and 5.9 Å, and 0.20 mM and 6.8 Å, respectively. Substrates or inhibitors were thus shown to move the n_1 and n_2 metal ion sites closer together. These data correlate well with other data that demonstrate substrate-induced conformational changes in the enzyme and synergism in substrate binding (*118–120*).

Experiments were conducted with CrADP that also show synergistic interaction between substrate sites. These Mn-to-Cr distances were 5.9, 5.2, and 4.8 Å with the CrADP, CrADP plus P_i, and CrADP, P_i plus glutamine complexes, respectively.

Data with substitution labile Co(II)-nucleotides were also obtained. Titrations with both Co(II)-ADP and Co(II)-ATP in the presence of the inhibitor methionine sulfoximine produced a diminution of the EPR spectrum of enzyme-bound Mn(II). The Co-to-Mn distances were 6.5 and 5.2 Å for the Co-ADP and Co-ATP complexes, respectively.

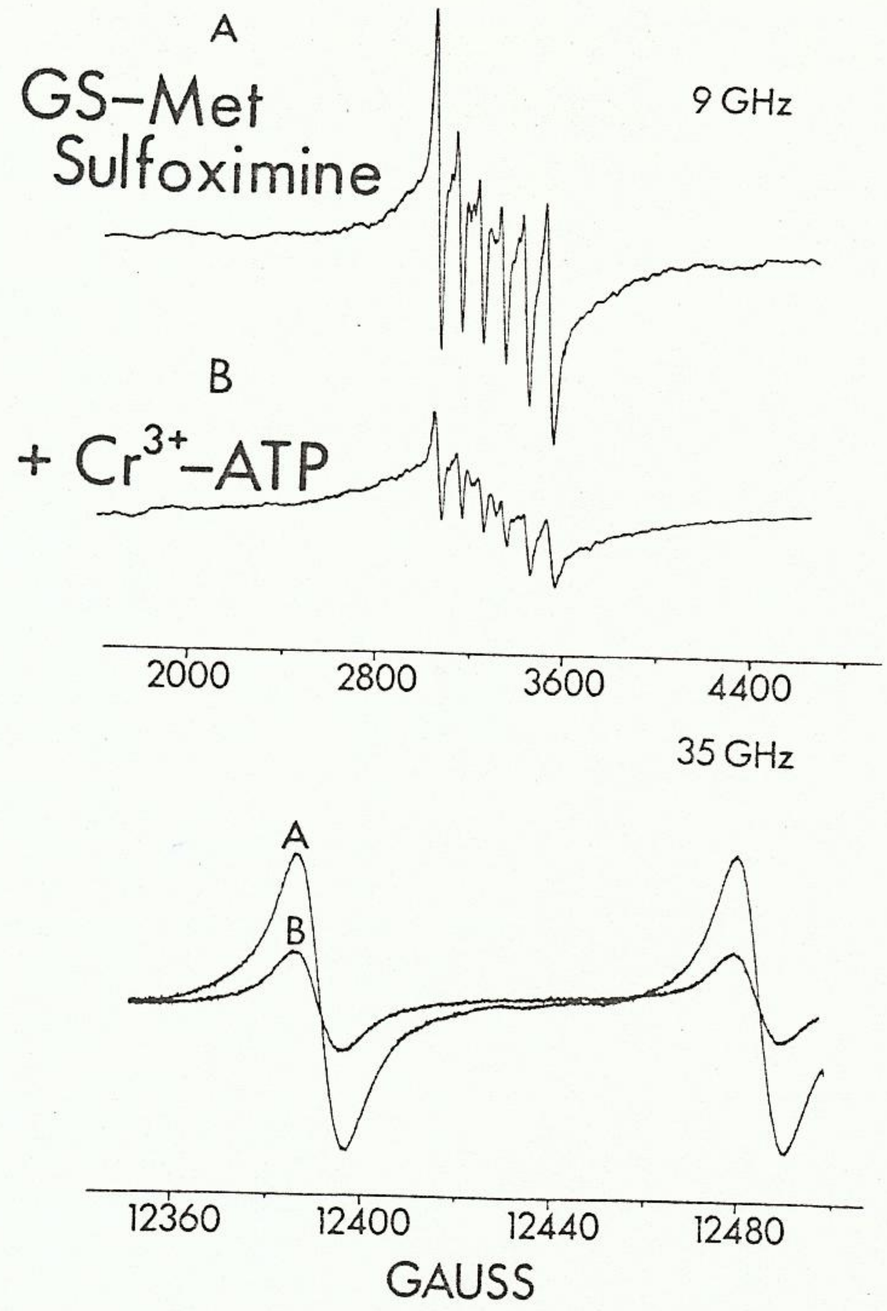

FIG. 25. EPR spectra showing the effect of Cr(III)-ATP binding on the spectrum of the glutamine synthetase-Mn(II)-methionine sulfoximine complex. Reprinted with permission of Academic Press from Villafranca *et al.* (*114*).

These data demonstrate a novel application of dipolar electron–electron relaxation between enzyme-bound metal ions for the determination of distances between the n_1 and n_2 metal ion sites of *E. coli* glutamine synthetase. The conclusion is that the two metal ions are in close enough proximity to both to be involved in substrate orientation, binding, and catalysis.

F. Distances between the Adenylyl Site and the Metal Ion Sites

Three physical methods, vis., NMR, EPR, and fluorescence energy transfer, were used to determine the spatial relationship between the adenylyl, catalytic (n_2), and the divalent metal ion activating sites (n_1). Glutamine synthetase of low adenylylation state ($E_{1.0}$) was enzymatically adenylylated with either [2-^{13}C] ATP, ε-ATP(1-N^6-etheno-ATP), or 6-amino-TEMPO-ATP (*121*, *122*).

Paramagnetic effects on the $1/T_1$ and $1/T_2$ relaxation rates of ^{13}C and ^{31}P nuclei of adenylylated glutamine synthetase ([2-^{13}C]AMP-GS) were measured when the two enzyme-bound Mg^{2+} ions were replaced by Mn^{2+} (*121*). Also the paramagnetic effects of Co^{2+} were measured on the ^{31}P relaxation rates of adenylylated enzyme. Distances between these metal ions and the ^{13}C and ^{31}P nuclei are summarized in Fig. 26.

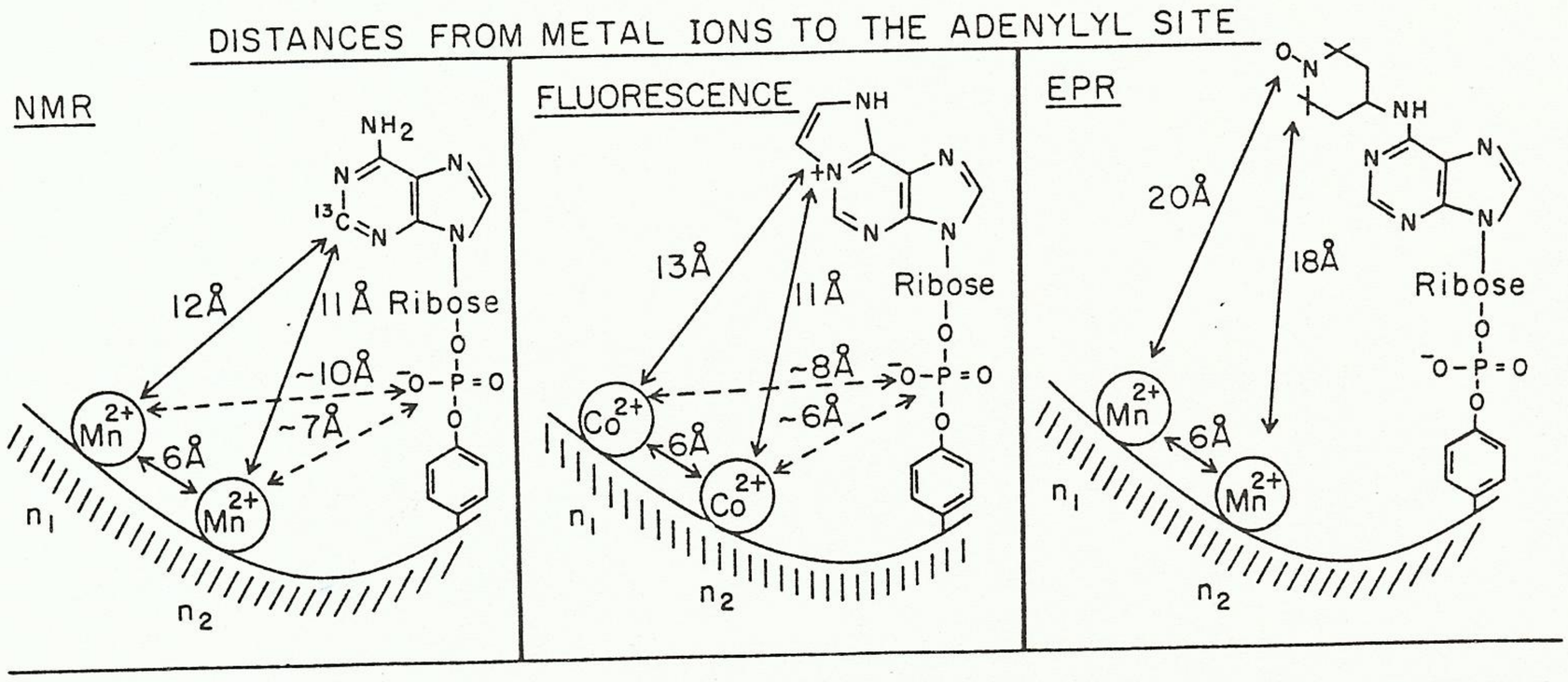

FIG. 26. Summary of [^{13}C], [^{31}P]-NMR data, fluorescence energy transfer data and EPR data on various derivatives at the covalent adenylyl site on glutamine synthetase. Reprinted with permission of Academic Press from Villafranca *et al.* (*115*).

Figure 26 also depicts the distances calculated from fluorescence quenching experiments by enzyme-bound Co^{2+} on the ε-adenosine moiety of ε-ATP adenylylated glutamine synthetase (ε-AMP-GS). Additional data were gathered by an EPR method that measured the decrease in EPR amplitude of the nitroxide spin-labeled adenylylated enzyme (TEMPO-AMP-GS) owing to enzyme-bound Mn^{2+} (*122*). Distances between Mn^{2+} and the N–O of the spin label are also shown in Fig. 26.

Thus, we have determined the distances between the adenylyl moiety and the two divalent metal ion binding sites on glutamine synthetase by ^{13}C and ^{31}P NMR, spin-labeled EPR, and fluorescence energy transfer methods. The results obtained from each method are in good agreement. The data show that the adenylyl regulatory site is close to the catalytic site (12–20 Å). Additional data on the rotational correlation time of the adenyl derivatives reveal that the adenylyl site is located on the surface of the enzyme.

G. NMR Studies of Distances to the Feedback Modifier Regulatory Sites and the Glutamate Site

As mentioned earlier in this article, the catalytic activity of glutamine synthetase is modulated by feedback inhibition as well as adenylylation. Stopped-flow fluorescence and NMR techniques have been used to study whether some of the feedback modifiers bind to the active site or to separate sites on the enzyme (*123*, *124*). The binding constants of L-glutamate, L-alanine, D-valine, and glycine were evaluated for Mg^{2+}-activated unadenylylated glutamine synthetase in the absence or presence of ATP or ADP and NH_3. Strong synergistic effects are noted when nucleotides are present, resulting in tighter binding of the amino acids. An analysis of the fluores-

cence data predicted a *decrease* in fluorescence intensity when L-ala was added to the enzyme L-glutamate complex if the feedback modifier displaced L-glutamate from the active site. However, the experimental data demonstrate an *increase* in fluorescence, and thus the data are consistent with a model wherein both L-ala and L-glutamate can bind to the enzyme simultaneously. Similar analyses with other amino acid pairs show that the following amino acids can simultaneously bind to the enzyme: L-glutamate-D-valine, L-alanine-D-valine, L-alanine-glycine, L-alanine-D-alanine. Other data show that D-alanine and D-valine bind to the same allosteric site and that glycine can bind to both the L-alanine and D-alanine sites.

NMR data are also consistent with L-alanine and L-glutamate binding to the enzyme simultaneously (*125*, *126*). In one experiment enzyme-Mn_2-ADP-L-glutamate was titrated with L-alanine. The paramagnetic effect of Mn^{2+} on the $1/T_1$ values for the protons of L-glutamate was essentially unchanged as L-alanine bound to the enzyme. Other calorimetric experiments with the L-alanine-L-glutamate pair also support the hypothesis that the L-glutamate substrate site is distinct from the L-alanine allosteric site (*125*). All of these experiments are in contradistinction to the earlier hypothesis of Dahlquist and Purich (*126*) which states that the feedback modifiers simply function by binding to the substrate site.

From the paramagnetic contribution to the $1/T_1$ value of the methyl

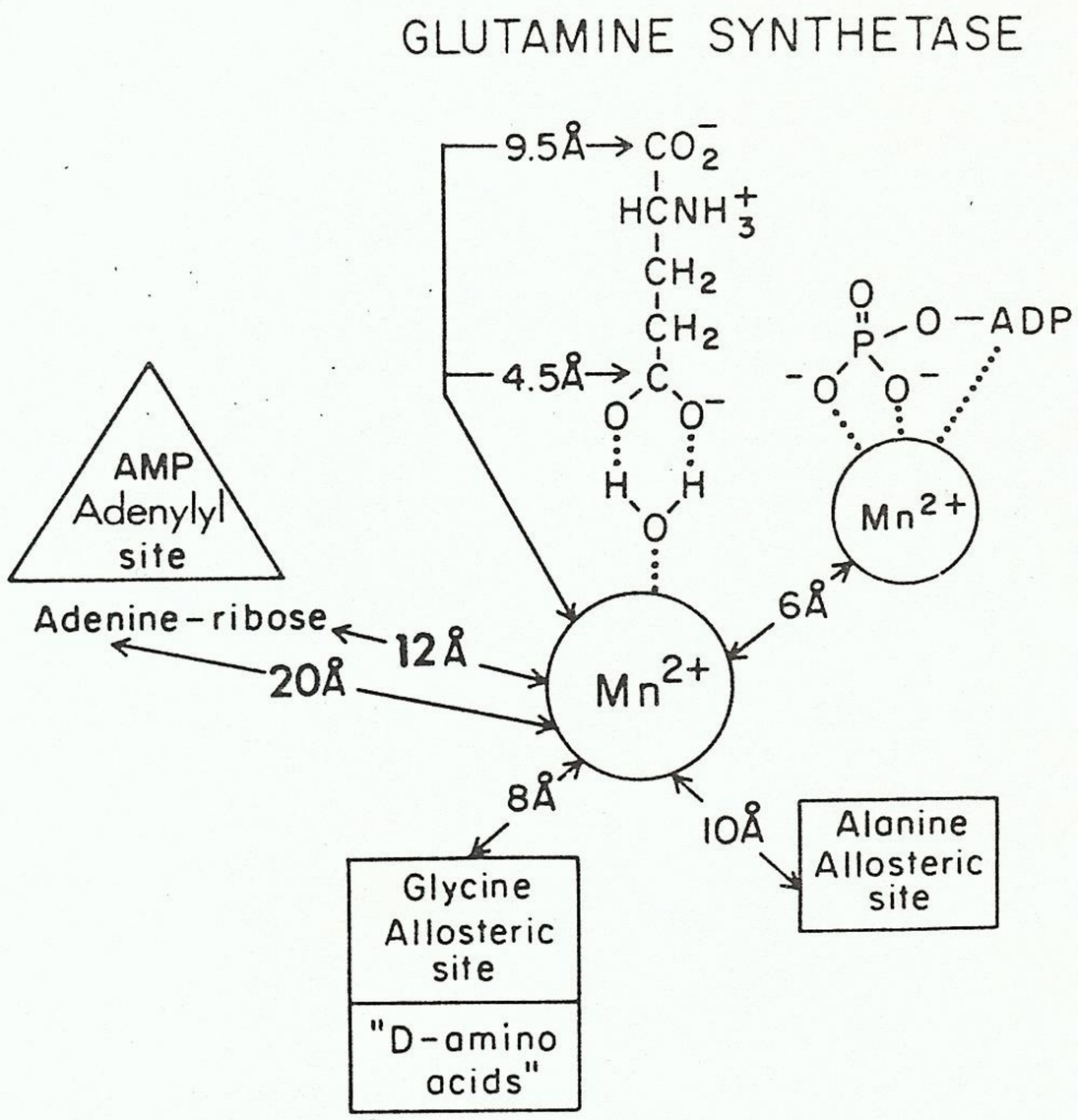

FIG. 27. Spatial relationships among the metal ion-substrate-adenylyl-feedback modifier sites on glutamine synthetase from *E. coli*.

group of L-alanine in the enzyme-$(Mn)_2$-ADP-L-alanine complex, a Mn-to-CH_3 distance of $\sim$10 Å was calculated. Similar data were gathered on the α-CH, β-CH_2, and γ-CH_2 protons of L-glutamate, and these distances are 8.0, 7.4, and 7.0 Å respectively (*124*). Distances from Mn^{2+} at the n_1 site and the two carboxyl groups of L-glutamate (^{13}C data) are given in Fig. 27. Likewise, Fig. 27 also includes preliminary distances from Mn^{2+} to the glycine and D-amino acid site (*124*).

H. Conclusions

This section summarizes recent data obtained from biophysical techniques on the nature of the metal ion, catalytic, and modifier sites of *E. coli* glutamine synthetase. Distance relationships between these sites are given in Fig. 27. This enzyme has many diverse modes of biochemical control. Recent data presented in this review demonstrate that progress is being made toward understanding the structural basis for the control of enzymic catalysis. When x-ray data become available (*127*), the amino acid groups at the catalytic site will be known and will provide further details concerning the mechanism of the enzymic reaction.

Acknowledgments

Support for part of this research was obtained from the National Science Foundation (PCM-78-07845) and the Public Health Service (GM-23529, AM-21785).

References

1. Dwek, R. A., "Nuclear Magnetic Resonance in Biochemistry." Oxford Univ. Press (Clarendon), London and New York, 1973.
2. Hirs, C. H. W., and Timasheff, S. N., eds., "Methods in Enzymology," Vol. 48. Academic Press, New York, 1978.
3. Hirs, C. H. W., and Timasheff, S. N., eds., "Methods in Enzymology," Vol. 49. Academic Press, New York, 1978.
4. Latt, S. A., Holmquist, B., and Vallee, B. L., *Biochem. Biophys. Res. Commun.* **37,** 333–339 (1969).
5. Feder, J., *Biochemistry* **6,** 2088–2093. (1967).
6. Pangburn, M. K., and Walsh, K. A., *Biochemistry* **14,** 4050–4054 (1975).
7. Feder, J., Brougham, L. R., and Wildi, B. S., *Biochemistry* **13,** 1186–1195 (1974).
8. Titani, K., Hermodson, M. A., Ericsson, L. H., Walsh, K. A., and Neurath, H., *Nature* (*London*), *New Biol.* **238,** 35–36 (1972).
9. Pangburn, M. K., Burstein, Y., Morgan, P. H., and Walsh, K. A., *Biochem. Biophys. Res. Commun.* **54,** 371–378 (1973).
10. Kester, W. R., and Matthews, B. W., *Biochemistry* **16,** 2506–2516 (1977).
11. Weaver, L. H., Kester, W. R., and Matthews, B. W., *J. Mol. Biol.* **114,** 119–132 (1977).
12. Holmquist, B., and Vallee, B. L., *J. Biol. Chem.* **249,** 4601–4607 (1974).

13. Holmquist, B., Kaden, T. A., and Vallee, B. L., *Biochemistry* **19,** 1454–1461 (1975).
14. Ishly, J., and Horrocks, W. DeW., *J. Inorg. Biochem.*, in press (1980).
15. Kennedy, F. S., Hill, H. A. O., Koden, T. A., and Vallee, B. L., *Biochem. Biophys. Res. Commun.* **48,** 1533–1539 (1972).
16. Horrocks, W. DeW., Holmquist, B., and Vallee, B. L., *Proc. Natl. Acad. Sci. U.S.A.* **72,** 4764–4768 (1975).
17. Horrocks, W. DeW., and Sudnick, D. R., *J. Am. Chem. Soc.* **101,** 334 (1979).
18. Bigbee, W. L., and Dahlquist, F. W., *Biochemistry* **13,** 3542–3549 (1974).
19. Bigbee, W. L., and Dahlquist, F. W., *Biochemistry* **16,** 3798–3803 (1978).
20. Pringle, J. R., *Biochem. Biophys. Res. Commun.* **39,** 46 (1970).
21. Schmidt, J. J., and Colowick, S. P., *Fed. Proc. Fed. Am. Soc. Exp. Biol.* **29,** 334 (1970).
22. Rustum, Y. M., Massaro, E. J., and Barnard, E. S., *Biochemistry* **10,** 3509 (1971).
23. Lazarus, N. R., Ramel, A. H., Rustum, Y. M., and Barnard, E. A., *Biochemistry* **5,** 4003 (1966).
24. Gazith, J., Schulze, I. T., Gooding, R. H., Womack, F. C., and Colowick, S. P., *Ann. N. Y. Acad. Sci.* **151,** 307 (1968).
25. Purich, D. L., Fromm, H. J., and Rudolph, F. B., *Adv. Enzymol.* **39,** 249 (1973).
26. Colowick, S. P., *in* "The Enzymes" (P. D. Boyer, ed.), 3rd ed., Vol. 9, p. 1. Academic Press, New York, 1973.
27. Sols, A., DelaFuente, G., Villar-Palasi, C., and Asensio, C., *Biochim. Biophys. Acta* **30,** 92 (1958).
28. Chen, M., and Whistler, R. L., *Arch. Biochem. Biophys.* **169,** 392 (1975).
29. Bessell, E. M., Foster, A. B., and Westwood, J. H., *Biochem. J.* **128,** 199 (1972).
30. Danenberg, K. D., and Cleland, W. W., *Biochemistry* **14,** 28 (1975).
31. Raushel, F. M., and Cleland, W. W., *J. Biol. Chem.* **248,** 8174 (1973).
32. Dills, W. L., and Meyer, W. L., *Biochemistry* **15,** 4506 (1976).
33. Raushel, F. M., and Cleland, W. W., *Biochemistry* **16,** 2169 (1977).
34. Salas, M., Vinuela, E., and Sols, A., *J. Biol. Chem.* **240,** 561 (1965).
35. Bailey, J. M., Fishman, P. H., and Pentcher, P. G., *J. Biol. Chem.* **243,** 4827 (1968).
36. Wurster, B., and Hess, B., *Eur. J. Biochem.* **36,** 68 (1973).
37. Raushel, F. M., unpublished observations.
38. Gabai, A., and Posternak, T., *Helv. Chim. Acta* **54,** 2141 (1971).
39. Hampton, A., and Slotin, L. A., *Biochemistry* **14,** 5438 (1975).
40. Hohnadel, D. C., and Cooper, C., *Biochemistry* **31,** 180 (1972).
41. Stahl, K., Schlimme, E., and Eckstein, F., *FEBS Lett.* **40,** 241 (1974).
42. Jaffee, E. K., and Cohn, M., *J. Biol. Chem.* **253,** 4823 (1978).
43. Cornelius, R. D., and Cleland, W. W., *Biochemistry* **17,** 3279 (1978).
44. Merritt, E. W., Sundaralingam, M., Cornelius, R. D., and Cleland, W. W., *Biochemistry* **17,** 3274 (1978).
45. Eigen, M., and Wilkins, R. G., *Adv. Chem. Ser* **49,** 55 (1968).
46. Cornelius, R. D., Hart, P. A., and Cleland, W. W., *Inorg. Chem.* **16,** 2799 (1977).
47. Eckstein, F., and Goody, R. S., *Biochemistry* **15,** 1685 (1976).
48. Pearson, R. G., *Science* **151,** 172 (1966).
49. Pearson, R. G., *J. Chem. Educ.* **45,** 581 (1968).
50. Bryant, F. R., and Benkovic, S. J., *Biochemistry* **18,** 2825 (1979).
51. Burgers, P. M. J., and Eckstein, F., *Proc. Natl. Acad. Sci. U.S.A.* **75,** 4798 (1978).
52. Cleland, W. W., *in* "The Enzymes" (P. D. Boyer, ed.), 3rd ed., Vol. 2, p. 1. Academic Press, New York, 1970.
53. Hammes, G. G., and Kochavi, D., *J. Am. Chem. Soc.* **84,** 2069 (1962).
54. Fromm, H. J., and Zewe, V., *J. Biol. Chem.* **237,** 3027 (1962).

55. Noat, G., Richard, J., Borel, M., and Got, C., *Eur. J. Biochem.* **5,** 55 (1968).
56. Rudolf, F. B., and Fromm, H. J., *J. Biol. Chem.* **246,** 6611 (1971).
57. Kosow, D. P., and Rose, I. A., *J. Biol. Chem.* **245,** 198 (1970).
58. Fromm, H. J., Silverstein, E., and Boyer, P. D., *J. Biol. Chem.* **239,** 3645 (1964).
59. Trayser, K. A., and Colowick, S. P., *Arch. Biochem. Biophys.* **94,** 161 (1961).
60. Kaji, A., and Colowick, S. P., *J. Biol. Chem.* **240,** 4454 (1965).
61. DelaFuente, G., Lagunas, R., and Sols, A., *Eur. J. Biochem.* **16,** 226 (1970).
62. Zewe, V., Fromm, H. J., and Fabiano, R., *J. Biol. Chem.* **239,** 1625 (1964).
63. Colowick, S. P., Womack, F. C., and Nielsen, J., *in* "The Role of Nucleotides for the Function and Conformation of Enzymes" (H. M. Kalckav, ed.), p. 15. Munksgaard, Copenhagen, 1969.
64. Noat, G., Ricard, J., Borel, M., and Got, C., *Eur. J. Biochem* **11,** 106 (1969).
65. Rose, I. A., O'Connell, E. L., Litwin, S., and Bar Tana, J., *J. Biol. Chem.* **249,** 5163 (1974).
66. Raushel, F. M., and Cleland, W. W., unpublished experiments.
67. Solheim, L. P., and Fromm, H. J., *174th Nat. Meet. Am. Chem. Soc., 1977* Abstract B10L-6 (1977).
68. Steitz, T. A., *J. Mol. Biol.* **61,** 695 (1971).
69. Steitz, T. A., Fletterick, R. J., and Hwang, K. J., *J. Mol. Biol.* **78,** 551 (1973).
70. Anderson, W. F., Fletterick, R. J., and Steitz, T. A., *J. Mol. Biol.* **86,** 261 (1974).
71. Fletterick, R. J., Bates, D. J., and Steitz, T. A., *Proc. Natl. Acad. Sci. U.S.A.* **72,** 38 (1975).
72. Anderson, W. F., and Steitz, T., *J. Mol. Biol.* **92,** 279 (1975).
73. Steitz, T. A., Anderson, W. F., Fletterick, R. J., and Anderson, C. M., *J. Biol. Chem.* **252,** 4494 (1977).
74. Anderson, C. M., McDonald, R. C., and Steitz, T. A., *J. Mol. Biol.* **123,** 1 (1978).
75. Anderson, C. M., Stenkamp, R. E., and Steitz, T. A., *J. Mol. Biol.* **123,** 15 (1978).
76. Anderson, C. M., Stenkamp, R. E., McDonald, R. C., and Steitz, T. A., *J. Mol. Biol.* **123,** 207 (1978).
77. Viola, R. E., and Cleland, W. W., *Fed. Proc., Fed. Am. Soc. Exp. Biol.* **37,** 1422 (1978).
78. Grouselle, M., Thiam, A., and Pudles, J., *Eur. J. Biochem.* **39,** 431 (1973).
79. Wohluether, R. M., Schutt, H., and Holtzer, H., *in* "The Enzymes of Glutamine Metabolism" (S. Prusiner and E. R. Stadtman, eds.), pp. 45–64. Academic Press, New York, 1973.
80. Meister, A., *in* "The Enzymes" (P. D. Boyer, ed.), 3rd ed., Vol. 10, pp. 699–754. Academic Press, New York, 1974.
81. Stadtman, E. R., and Ginsburg, A., *in* "The Enzymes" (P. D. Boyer, ed.), 3rd ed., Vol. 10, pp. 755–812. Academic Press, New York, 1974.
82. Ginsburg, A., (1972) *Adv. Protein Chem.* 27, 1–79 (1972).
83. Ginsburg, A., and Stadtman, E. R., *in* "The Enzymes of Glutamine Metabolism" (S. Prusiner and E. R. Stadtman, eds.), pp. 9–44. Academic Press, New York, 1973.
84. Tate, S. S., and Meister, A., *in* "The Enzymes of Glutamine Metabolism" (S. Prusiner and E. R. Stadtman, eds.), pp. 77–128. Academic Press, New York, 1973.
85. Wedler, F. C., and Boyer, P. D., *J. Biol. Chem.* **247,** 948–992 (1972).
86. Wedler, F. C., *J. Biol. Chem.* **249,** 5080–5087 (1974).
87. Wedler, F. C., and Horn, B. R., *J. Biol. Chem.* **251,** 7530–7538 (1976).
88. Allison, R. D., Todhunter, J. A., and Purich, D. L., *J. Biol. Chem.* **252,** 6046–6051 (1977).
89. Stokes, B. O., and Boyer, P. D., *J. Biol. Chem.* **251,** 5558–5564 (1976).
90. Balakrishnan, M. S., Sharp, T. R., and Villafranca, J. J., *Biochem. Biophys. Res. Commun.* **85,** 991–998 (1978).
91. Cohn, M., and Hu, A., *Proc. Natl. Acad. Sci. U.S.A.* **75,** 200–203 (1978).
92. Sleep, J. A., Hackney, D. D., and Boyer, P. D., *J. Biol. Chem.* **253,** 5232–5238 (1978).
93. Hackney, D. D., and Boyer, P. D., *Proc. Natl. Acad. Sci. U.S.A.* **75,** 3133–3137 (1978).

94. Timmons, R. B., Rhee, S. G., Luterman, D. C., and Chock, P. B., *Biochemistry* **13,** 4479–4485 (1974).
95. Midlefort, C. F., and Rose, I. A., *J. Biol. Chem.* **251,** 5881–5887 (1976).
96. Ronzio, R. A., Rowe, W. B., and Meister, A., *Biochemistry* **8,** 1066–1075 (1969).
97. Rowe, W. B., Ronzio, R. A., and Meister, A., *Biochemistry* **8,** 2674–2680 (1969).
98. Manning, J. M., Moore, S., Rowe, W. B., and Meister, A., *Biochemistry* **8,** 2681–2685 (1969).
99. Gass, J. D., and Meister, A., *Biochemistry* **9,** 842–846 (1970).
100. Khedouri, E., Wellner, V. P., and Meister, A., *Biochemistry* **3,** 824–828 (1964).
101. Tsuda, Y., Stephani, R. A., and Meister, A., *Biochemistry* **10,** 3186–3189 (1971).
102. Meister, A., *Adv. Enzymol.* **31,** 183–218 (1968).
103. Meister, A., *Harvey Lect.* **63,** 139 (1968).
104. Gass, J. D., and Meister, A., *Biochemistry* **9,** 1380–1389 (1970).
105. Wolfenden, R., *Acc. Chem. Res. 5,* 10–18 (1972).
106. Meek, T. D., and Villafranca, J. J., *Middle Atl. Reg. Meet. Am. Chem. Soc., 12th,* 1978 Abstract P55 (1978).
107. Meek, T. D., and Villafranca, J. J., in preparation.
108. Bayer, E., Gugel, K. H., Hägele, K., Hagenmaier, H., Jessipow, S., König, W. A., and Zähner, H., *Helv. Chim. Acta* **55,** 224–239 (1972).
109. Hunt, J. B., Smyrniotis, P. Z., Ginsburg, A., and Stadtman, E. R., *Arch. Biochem. Biophys.* **166,** 102–124 (1975).
110. Villafranca, J. J., and Wedler, F. C., *Biochemistry* **13,** 3286–3291 (1974).
111. Villafranca, J. J., and Ash, D. E., and Wedler, F. C., *Biochemistry* **15,** 536–544 (1976).
112. Shrake, A., Powers, D. M., and Ginsburg, A., *Biochemistry* **16,** 4372–4381 (1977).
113. Villafranca, J. J., Ash, D. E., and Wedler, F. C. *Biochemistry* **15,** 544–553 (1976).
114. Villafranca, J. J., Ash, D. E., and Wedler, F. C., *Biochem. Biophys. Res. Commun.* **66,** 1003–1010 (1975).
115. Villafranca, J. J., Balakrishnan, M. S., and Wedler, F. C., *Biochem. Biophys. Res. Commun.* **75,** 464–471 (1977).
116. Balakrishnan, M. S., and Villafranca, J. J., *Biochemistry* **17,** 3531–3538 (1978).
117. Leigh, J. S., *J. Chem. Phys.* **52,** 2608–2612 (1970).
118. Rhee, S. G., and Chock, P. B., *Biochemistry* **15,** 1755–1760 (1976).
119. Rhee, S. G., and Chock, P. B., *Proc. Natl. Acad. Sci. U.S.A.* **73,** 476–480 (1976).
120. Rhee, S. G., Chock, P. B., and Stadtman, E. R., *Biochimie* **58,** 35–49 (1976).
121. Villafranca, J. J., Rhee, S. G., and Chock, P. B., *Proc. Natl. Acad. Sci. U.S.A.* **75,** 1255–1259 (1978).
122. Chock, P. B., Villafranca, J. J., Rhee, S. G., Ubom, G., and Stadtman, E. R., *in* "NMR and Biochemistry" (P. Lu and S. Opella, eds.), pp. 405–418. Marcel Dekker. New York, 1979.
123. Rhee, S. G., Villafranca, J. J., Chock, P. B., and Stadtman, E. R., *Biochem. Biophys. Res. Commun.* **78,** 244–250 (1977).
124. Villafranca, J. J., *in* "Biomolecular Structure and Function" (P. F. Agris, ed.), pp. 353–362. Academic Press, New York, 1978.
125. Shrake, A., Park, R., and Ginsburg, A., *Biochemistry* **17,** 658–664 (1978).
126. Dahlquist, F. W., and Purich, D. L., *Biochemistry* **14,** 1980–1989 (1975).
127. Kabsch, W., Kabsch, H., and Eisenberg, D., *J. Mol. Biol.* **100,** 283–291 (1976).